ANZIAM J. 59(2018), 370–401
doi:10.1017/S144618111700044X

DYNAMIC RELATIONSHIP BETWEEN THE MUTUAL INTERFERENCE AND GESTATION DELAYS OF A HYBRID TRITROPHIC FOOD CHAIN MODEL

RASHMI AGRAWAL[1], DEBALDEV JANA[2], RANJIT KUMAR UPADHYAY[3] and V. SREE HARI RAO[4]

(Received 12 May, 2016; accepted 12 April, 2017; first published online 26 February 2018)

Abstract

We have proposed a three-species hybrid food chain model with multiple time delays. The interaction between the prey and the middle predator follows Holling type (HT) II functional response, while the interaction between the top predator and its only food, the middle predator, is taken as a general functional response with the mutual interference schemes, such as Crowley–Martin (CM), Beddington–DeAngelis (BD) and Hassell–Varley (HV) functional responses. We analyse the model system which employs HT II and CM functional responses, and discuss the local and global stability analyses of the coexisting equilibrium solution. The effect of gestation delay on both the middle and top predator has been studied. The dynamics of model systems are affected by both factors: gestation delay and the form of functional responses considered. The theoretical results are supported by appropriate numerical simulations, and bifurcation diagrams are obtained for biologically feasible parameter values. It is interesting from the application point of view to show how an individual delay changes the dynamics of the model system depending on the form of functional response.

2010 *Mathematics subject classification*: primary 70K50; secondary 37C75, 65Q10, 74H65.

Keywords and phrases: CM functional response, BD functional response, HV functional response, gestation delay, multiple time delays, Hopf-bifurcation, chaos.

1. Introduction

In mathematical models of interacting population, one of the important elements is the functional response, which mostly determines the dynamics of a system [21].

[1]Department of Humanities and Science, S R Engineering College, Warangal, Telangana 506371, India; e-mail: agrawal.rashmi2@gmail.com.
[2]Department of Mathematics and SRM Research Institute, SRM Institute of Science and Technology, Kattankulathur 603203, Tamil Nadu, India; e-mail: debaldevjana.jana@gmail.com.
[3]Department of Applied Mathematics, Indian Institute of Technology (ISM), Dhanbad, Jharkhand 826004, India; e-mail: ranjit.chaos@gmail.com.
[4]CEO, Turnin Innovation Technologies (Pvt) Ltd, Hyderabad, India; e-mail: vshrao@turnin.in.

There are many significant functional responses to model various ecological situations, and one of them is the mutual interference. It is the behavioural interaction among feeding organisms that reduce the time each individual spends obtaining food or the amount of food each individual consumes. Nonspatial factors which can influence the functional response are direct interferences between predator, fission or fusion of groups, cooperative hunting in groups and adaptive foraging [3]. A number of mechanisms involving the spatial distribution of predators, prey or opportunities for predation can lead to a predator-dependent functional response. Skalski and Gilliam [25] show statistical evidences from 19 prey–predator systems that the models with predator-dependent functional responses (Hassell–Varley (HV) [14], Beddington–DeAngelis (BD) [2, 5] and Crowley–Martin (CM) [4]), can provide better description of predator feeding over a range of prey–predator abundances. Contemporary theoretical works have documented that mathematical forms of the feeding rates can influence the distribution of predators among the space [19], the stability of enriched prey–predator systems [5, 15], the length of food chains [24], correlations between nutrient enrichment, and the biomass of higher trophic levels [5]. Also the predator-dependent functional response predicts asymptotic feeding rates at high prey abundance that are independent of predator abundance (for example, the model with BD and HV functional response), but others predict an asymptotic nature that depends on the density of predators (for example, the model with CM functional response) [25]. In the literature, we find several works for various purposes and uses of HV [22, 30], BD [1, 16] and CM [28, 29] functional responses which show significant dynamical characteristics due to the predator interference and these results differ from the conventional Volterra scheme.

After predation, some amounts of energy (biomass) of the prey individuals assimilate into the predator's energy (biomass). The assimilation process is completed through various bio-physiological processes, such as predation, digestion, absorption and so on. After entering into the predator's body, the raw food is finally transformed into the predator's energy in the form of biomass. Such a transformation process requires time. Therefore, it would be more realistic to consider a time delay in the predator's gestation process (that is, in the growth term of the predator's population) [18, 23]. One of the most important and significant factors among the food web structure in population ecology is time delay, which is observed in almost every biological process. In general, time delays make the systems more complex but realistic. In addition, varying time delays make the system exhibit rich dynamics. Kuang [18] has explained that animals must take some time to digest their food. A brief review on prey–predator models with discrete delay (as gestation) for both Kolmogorov and non-Kolmogorov types of model systems are presented by Ruan [23], where one can find different mathematical criteria for different biological assumptions due to delay. Discrete time delays with different biological meanings in hybrid food chain models are well-studied [1, 16], and many interesting dynamical features including chaos are observed. It is well-documented that biological and/or environmental processes, such as the Allee effect [20], omnivory [27],

https://doi.org/10.1017/S144618111700044X Published online by Cambridge University Press

latency in biological processes [8, 26], large turnover of resource [32], coupling of incommensurate oscillations [11], seasonal forcing [7, 10], noise [6, 9] and so on, may produce chaos. Time delay plays a challenging role in food chain models, either to induce chaos [1] or settle down the system from chaos to regular dynamics [1].

The interference of predators in their predation and assimilation process, and the time required for assimilation are very important factors for any food chain model. These factors play a crucial role in the understanding of a food web. Dynamical diversities come through different choices of the predator's interference on their foraging strategies, and also the time delay is a significant contributing factor for introducing oscillations. The present research explores the interplay of various functional responses that exist in the literature and are useful to understand the phenomena of competition among various species. Most mathematical models proposed to study the dynamics of interacting species remain generic, since it is not possible to suggest the type of functional response that suits the type of species in nature. This is a question of vital importance from the theoretical as well as experimental points of view, which may be achieved with the help of the biologists involved in experimental studies. We hope that the present work, being exhaustive and having the theoretical strength of considering various types of response functions, paves the way for true and more meaningful collaborative research with experimental biologists in order to identify satisfactory answers to the above mentioned question of importance. Further, the exploratory results of the present study would help initiate future work in this direction, besides being a valuable addition to the literature from this point of view.

The rest of the paper is organized as follows. In the next section, we present a mathematical formulation of the model system, and the preliminary results such as positive invariance, boundedness of solutions, analysis of equilibria are discussed. In Section 3, we perform the local stability and Hopf-bifurcation analysis around the interior equilibrium point in all possible cases. Conditions for the existence of global stability of the interior equilibrium point is also derived in this section. In Section 4, the formulae to determine the properties of the Hopf-bifurcating periodic solutions are derived by applying the normal form theory and central manifold theorem. Numerical simulations are performed to substantiate our analytical results and to study the dynamic behaviour of all three functional responses, showing the mutual interference scheme in Section 5. Finally, we summarize our results and conclude our findings in Section 6. All appendices are included in the Supplementary material. Supplementary material is available at doi:10.1017/S144618111700044X.

2. The mathematical model

We consider the following system of equations as a mathematical model to describe a hybrid tritrophic food chain interaction, where $X(T), Y(T), Z(T)$ denote the population densities of the lowest trophic level species (prey), the middle trophic level species (intermediate predator) and the highest trophic level species (top predator),

respectively, at time T:

$$\begin{aligned}\frac{dX}{dT} &= a_1X\left(1-\frac{X}{K}\right)-\frac{\omega_0XY}{X+D},\\ \frac{dY}{dT} &= -a_2Y+\frac{\omega_1XY}{X+D_1}-\omega_2f(Y,Z),\\ \frac{dZ}{dT} &= -a_3Z+\omega_3f(Y,Z).\end{aligned} \tag{2.1}$$

In this model, we assume that the prey population grows logistically. The interaction between the prey and an intermediate predator follows HT II functional response, while that between the top predator and its prey is taken as a general functional response $f(Y,Z)$, which corresponds to any of the functional responses with mutual interference schemes between the species Y and Z. First, we consider $f(Y,Z)$ as a CM type functional response and study the dynamics of the model system. Further, we also discuss the dynamics of the system by considering $f(Y,Z)$ as BD type and HV type functional responses, respectively. Therefore, we discuss the model which employs HT II and CM type functional responses. We assume that there is a gestation delay in the predator, that is, after consumption of prey, the predator requires some time to assimilate the density of prey. Therefore, we assume that the change rate of the predator depends on the numbers of prey and predators present at some previous time. Since both the predators (intermediate-Y and top-Z) are different by bio-physiological processes, we are considering two different discrete gestation delays $T_1, T_2 > 0$ for both intermediate and top predators, respectively. So, the model system (2.1) becomes:

$$\begin{aligned}\frac{dX}{dT} &= a_1X\left(1-\frac{X}{K}\right)-\frac{\omega_0XY}{X+D},\\ \frac{dY}{dT} &= -a_2Y+\frac{\omega_1X(T-T_1)Y(T-T_1)}{X(T-T_1)+D_1}-\frac{\omega_2YZ}{1+dY+bZ+bdYZ},\\ \frac{dZ}{dT} &= -a_3Z+\frac{\omega_3Y(T-T_2)Z(T-T_2)}{1+dY(T-T_2)+bZ(T-T_2)+bdY(T-T_2)Z(T-T_2)}.\end{aligned} \tag{2.2}$$

The prey X grows with intrinsic per capita growth rate a_1 and carrying capacity K in the absence of predation. The parameters D and D_1 measure the extent to which the environment provides protection to prey X and intermediate predator Y, respectively, and ω_0 is the maximum value that the per capita reduction rate of X can attain. The expression ω_1/ω_0 represents the conversion rate of the consumed prey. The constants ω_2, ω_3, b and d are the saturating CM type functional response parameters, in which b and d measure the magnitude of interference among top and intermediate predators, respectively. Further, a_2 and a_3 are the death rates of the intermediate and top predators, respectively. All model parameters assume only positive values. Obviously, model system (2.2) is a three-species simple food chain model involving a hybrid type of prey-dependent and predator-dependent functional responses.

https://doi.org/10.1017/S144618111700044X Published online by Cambridge University Press

Now, introducing the variables $x = X/K, y = \omega_0 Y/a_1 K, z = \omega_0\omega_2 Z/{a_1}^2 dK$ and $t = a_1 T, T_1 = a_1\tau_1, T_2 = a_1\tau_2$, we obtain the following dimensionless system

$$\begin{aligned}
\frac{dx}{dt} &= x(1-x) - \frac{xy}{x+\omega_4},\\
\frac{dy}{dt} &= -\omega_5 y + \frac{\omega_6 x(t-\tau_1)y(t-\tau_1)}{x(t-\tau_1)+\omega_7} - \frac{yz}{y+(\omega_8+\omega_9 y)z+\omega_{10}},\\
\frac{dz}{dt} &= -\omega_{11} z + \frac{\omega_{12} y(t-\tau_2)z(t-\tau_2)}{y(t-\tau_2)+(\omega_8+\omega_9 y(t-\tau_2))z(t-\tau_2)+\omega_{10}},
\end{aligned} \tag{2.3}$$

where the dimensionless parameters are given by $\omega_4 = D/K$, $\omega_5 = a_2/a_1$, $\omega_6 = \omega_1/a_1$, $\omega_7 = D_1/K$, $\omega_8 = a_1 b/\omega_2$, $\omega_9 = a_1^2 bdK/\omega\omega_2$, $\omega_{10} = \omega/a_1^2 dK$, $\omega_{11} = a_3/a_1$, $\omega_{12} = \omega_3/a_1 d$; all these parameters are positive. The initial conditions of (2.3) are

$$\begin{aligned}
&x(\theta) = \phi_1(\theta) \geq 0, \quad y(\theta) = \phi_2(\theta) \geq 0, \quad z(\theta) = \phi_3(\theta) \geq 0,\\
&\text{with } \theta \in [-\tau, 0], \quad \phi_i(0) > 0 \quad (i = 1, 2, 3).
\end{aligned} \tag{2.4}$$

Here $\tau = \max[\tau_1, \tau_2]$ and $\phi : [-\tau, 0] \to \Re^3$, such that $\phi = (\phi_1, \phi_2, \phi_3)$, is continuous with norm

$$\|\phi\| = \sup_{-\tau\leq\theta\leq 0} \{|\phi_1(\theta)|, |\phi_2(\theta)|, |\phi_3(\theta)|\}.$$

By the fundamental theory of functional differential equations [12], there is a unique solution $(x(t), y(t), z(t))$ to system (2.3) with initial conditions (2.4).

Biologically, positivity ensures that population never become negative and always survives [17]. Using the lemma of Yang et al. [31, Lemma 4], it is obvious that all solutions of (2.3) with initial conditions (2.4) are positive. Also, the boundedness may be interpreted as a natural restriction to growth as a consequence of limited resources [17]. For any positive solution $\phi(t) = (x(t), y(t), z(t))$ of the system (2.3), there exists a $\tilde{T} > 0$, such that $0 \leq x(t) \leq M_1$, $0 \leq y(t) \leq M_2$ and $0 \leq z(t) \leq M_3$ for $t > \tilde{T}$, where

$$M_1 = 1, \quad M_2 = \frac{\omega_6}{4\omega_5}, \quad M_3 = \frac{M_2\omega_{12}}{\omega_{11}(m_2\omega_9 + \omega_8)}$$

(see Appendix A.1 in Supplementary material). The model system (2.3) has four nonnegative equilibria given as: (i) $E_0(0, 0, 0)$, (ii) $E_1(1, 0, 0)$, (iii) $E_2(\tilde{x}, \tilde{y}, 0)$, where $\tilde{x} = \omega_5\omega_7/(\omega_6 - \omega_5)$, $\tilde{y} = (1 - \tilde{x})(\tilde{x} + \omega_4)$, provided that $0 < \omega_5\omega_7/(\omega_6 - \omega_5) < 1$ with $\omega_6 > \omega_5$ and (iv) $E^*(x^*, y^*, z^*)$ where, $y^* = (1 - x^*)(x^* + \omega_4)$, $z^* = ((\omega_{12} - \omega_{11})y^* - \omega_{10}\omega_{11})/(\omega_{11}(\omega_8 + \omega_9 y^*))$, such that $0 < x^* < 1$ and $0 < \omega_{10}\omega_{11}/(\omega_{12} - \omega_{11}) < y^*$ with $\omega_{12} > \omega_{11}$. Detailed stability analysis of delay free model system (2.3) was discussed by Upadhyay and Naji [28]. Here, we study the stability analysis of the coexisting equilibrium point for a delayed model system (2.3).

3. Local stability analysis and Hopf-bifurcation

Let $E^*(x^*, y^*, z^*)$ be a positive equilibrium point of the model system (2.3). The Jacobian matrix evaluated at E^* yields the characteristic equation

$$\det(A_1 + e^{-\lambda\tau_1}A_2 + e^{-\lambda\tau_2}A_3 - \lambda I_3) = 0, \tag{3.1}$$

https://doi.org/10.1017/S144618111700044X Published online by Cambridge University Press

where I_3 is an identity matrix of order 3 and

$$A_1 = \frac{\partial F(W)}{\partial W(t)} = \begin{pmatrix} -x^*\left(1 - \dfrac{y^*}{\alpha^2}\right) & -\dfrac{x^*}{\alpha} & 0 \\ 0 & -\omega_5 - \dfrac{z^*(\omega_8 z^* + \omega_{10})}{\gamma^2} & -\dfrac{y^*(y^* + \omega_{10})}{\gamma^2} \\ 0 & 0 & -\omega_{11} \end{pmatrix},$$

$$A_2 = \frac{\partial F(W)}{\partial W(t-\tau_1)} = \begin{pmatrix} 0 & 0 & 0 \\ \dfrac{\omega_6\omega_7 y^*}{\beta^2} & \dfrac{\omega_6 x^*}{\beta} & 0 \\ 0 & 0 & 0 \end{pmatrix},$$

$$A_3 = \frac{\partial F(W)}{\partial W(t-\tau_2)} = \begin{pmatrix} 0 & 0 & 0 \\ 0 & 0 & 0 \\ 0 & \dfrac{\omega_{12} z^*(\omega_8 z^* + \omega_{10})}{\gamma^2} & \dfrac{\omega_{12} y^*(y^* + \omega_{10})}{\gamma^2} \end{pmatrix},$$

with $\alpha = x^* + \omega_4, \beta = x^* + \omega_7$ and $\gamma = y^* + (\omega_8 + \omega_9 y^*)z^* + \omega_{10}$. From equation (3.1), the characteristic equation of the model (2.3) is given as follows:

$$\lambda^3 + A\lambda^2 + B\lambda + C + e^{-\lambda\tau_1}(D\lambda^2 + E\lambda + F) + e^{-\lambda\tau_2}(G\lambda^2 + H\lambda + I) + e^{-\lambda(\tau_1+\tau_2)}(J\lambda + K) = 0, \tag{3.2}$$

where

$$A = -(a_{11} + a_{22} + a_{33}), \quad B = a_{11}a_{22} + a_{11}a_{33} + a_{22}a_{33}, \quad C = -a_{11}a_{22}a_{33},$$
$$D = -b_{22}, \quad E = a_{33}b_{22} + a_{11}b_{22} - a_{12}b_{21}, \quad F = a_{12}a_{33}b_{21} - a_{33}a_{11}b_{22}, \quad G = -c_{33},$$
$$H = a_{22}c_{33} + a_{11}c_{33} - a_{23}c_{32}, \quad I = a_{11}a_{23}c_{32} - a_{11}a_{22}c_{33}, \quad J = b_{22}c_{33},$$
$$K = a_{12}b_{21}c_{33} - a_{11}b_{22}c_{33},$$

such that $A_1 = a_{ij}|_{i,j=1,2,3}$, $A_2 = b_{ij}|_{i,j=1,2,3}$ and $A_3 = c_{ij}|_{i,j=1,2,3}$. We now discuss the following cases.

Case I: $\tau_1 = 0 = \tau_2$.
In this case, equation (3.2) reduces to

$$\lambda^3 + \mu_1\lambda^2 + \mu_2\lambda + \mu_3 = 0, \tag{3.3}$$

where $\mu_1 = A + D + G, \mu_2 = B + E + H + J, \mu_3 = C + F + I + K$. By Routh–Hurwitz's criterion, $E^*(x^*, y^*, z^*)$ is locally asymptotically stable, if μ_1, μ_3 and $\Delta = \mu_1\mu_2 - \mu_3$ are positive. It gives the following conditions for E^* to be locally asymptotically stable:

$$\mu_1 > 0 \Rightarrow \frac{x^*y^*}{\alpha^2} + \frac{y^*z^*(1 + \omega_9 z^*)}{\gamma^2} \leq x^*, \tag{3.4}$$

$$\mu_2 > 0 \Rightarrow \omega_6\omega_7\alpha\gamma^2 + y^*z^*\beta^2(1 + \omega_9 z^*) \geq z^*\alpha^2\beta^2(1 + \omega_9 z^*), \tag{3.5}$$

$$\Delta > 0 \Rightarrow \omega_{12}(\omega_8 + \omega_9 y^*) > (1 + \omega_9 z^*). \tag{3.6}$$

Case II: $\tau_1 \neq 0$ and $\tau_2 = 0$.
In this case, equation (3.2) becomes

$$\lambda^3 + (A + G)\lambda^2 + (B + H)\lambda + (C + I) + e^{-\lambda\tau_1}(D\lambda^2 + (E + J)\lambda + (F + K)) = 0. \tag{3.7}$$

https://doi.org/10.1017/S144618111700044X Published online by Cambridge University Press

Let $i\omega$ ($\omega > 0$) be a root of equation (3.7). Then,

$$-\omega^3 + \omega(B+H) = (-D\omega^2 + F + K)\sin\omega\tau_1 - \omega(E+J)\cos\omega\tau_1 \tag{3.8}$$

$$-\omega^2(A+G) + (C+I) = (D\omega^2 - F - K)\cos\omega\tau_1 - \omega(E+J)\sin\omega\tau_1. \tag{3.9}$$

Squaring and adding equations (3.8) and (3.9), we get

$$\omega^6 + \hat{a}\omega^4 + \hat{b}\omega^2 + \hat{c} = 0, \tag{3.10}$$

where

$$\hat{a} = [(A+G)^2 - 2(B+H) - D^2],$$
$$\hat{b} = [(B+H)^2 - 2(A+G)(C+I) + 2D(F+K) - (E+J)^2],$$
$$\hat{c} = (C+I)^2 - (F+K)^2.$$

Now, we define

$$F(\omega) = \omega^6 + \hat{a}\omega^4 + \hat{b}\omega^2 + \hat{c} = 0$$

and assume that

$$(C+I)^2 - (F+K)^2 < 0. \tag{3.11}$$

Then, note that $F(0) < 0$ and $F(\infty) = \infty$. Thus, equation (3.10) has a finite number of positive roots, say $\omega_1, \omega_2, \ldots, \omega_k$. For every fixed $\omega_i, i = 1, 2, \ldots, k$, there exist a sequence $\{\tau_{1_i}^j | j = 1, 2, \ldots\}$, such that

$$\tau_{1_i}^j = \frac{1}{\omega_i}\cos^{-1}\left[\frac{\Upsilon}{\Omega}\right] + \frac{2j\pi}{\omega_i}, \tag{3.12}$$

where $i = 1, 2, \ldots, k$; $j = 0, 1, 2 \ldots$ and

$$\Upsilon = \omega_i^4(E+J) - \omega_i^2(B+H)(E+J) - (-D\omega_i^2 + F + K)(-\omega_i^2(A+G) + (C+I)),$$
$$\Omega = (-D\omega_i^2 + F + K)^2 + \omega_i^2(E+J)^2.$$

Let $\tau_{1_0} = \min\{\tau_{1_i}^j \mid i = 1, 2, \ldots, k; j = 0, 1, 2, \ldots\}$. We also obtain

$$\left\{\frac{d}{d\tau_1}\mathrm{Re}(\lambda)\right\}_{\tau_1=\tau_{1_0}} = \frac{\eta_1\rho_1 - \eta_2\rho_2}{\Lambda} > 0,$$

provided $\eta_1\rho_1 - \eta_2\rho_2 > 0$, where

$$\Lambda = (\omega_i(F+K) - \omega_i^3 D)^2 + \omega_i^4(E+J)^2,$$
$$\eta_1 = (-3\omega_i^2 + B + H)\sin\omega_i\tau_1 + 2\omega_i(A+G)\cos\omega_i\tau_1 + 2\omega_i D,$$
$$\eta_2 = (-3\omega_i^2 + B + H)\cos\omega_i\tau_1 - 2\omega_i(A+G)\sin\omega_i\tau_1 + (E+J),$$
$$\rho_1 = \omega_i(F+K) - \omega_i^3 D, \quad \rho_2 = \omega_i^2(E+J).$$

Then, by the general Hopf-bifurcation theorem [18], we have the following result on the stability and bifurcation of the system (2.3).

THEOREM 3.1. *Assume the conditions* (3.4)–(3.6) *and* (3.11) *hold. Then the equilibrium* $E^*(x^*, y^*, z^*)$ *is locally asymptotically stable for* $\tau_1 < \tau_{1_0}$ *and unstable for* $\tau_1 > \tau_{1_0}$. *Furthermore, the system* (2.3) *undergoes a Hopf-bifurcation at* $E^*(x^*, y^*, z^*)$ *when* $\tau_1 = \tau_{1_0}$.

https://doi.org/10.1017/S144618111700044X Published online by Cambridge University Press

Case III: $\tau_1 \in (0, \tau_{1_0}), \tau_2 \neq 0$.
In this case, we allow a gestation time period for the top predator and also a constant gestation time delay for the middle predator. We fix $\tau_1 = \tilde{\tau}_1$ at some value from its stability range $(0, \tau_{1_0})$ and regard τ_2 as a free parameter. We also assume that the model parameters are such that the conditions (3.4)–(3.6) hold. Let $i\omega$ with $\omega > 0$ be a root of equation (3.2). Then,

$$\omega^6 + \tilde{a}\omega^4 + \tilde{b}\omega^2 + 2\tilde{c}\sin\omega\tau_1 + 2\tilde{d}\cos\omega\tau_1 + \tilde{e} = 0, \tag{3.13}$$

where

$$\begin{aligned}
\tilde{a} &= A^2 + D^2 - G^2 - 2B,\\
\tilde{b} &= B^2 - 2DF + E^2 - 2AC + 2GI - H^2 - J^2,\\
\tilde{c} &= -AE\omega^3 + CE\omega + \omega^3(-D\omega^2 + F) - B\omega(-D\omega^2 + F) - J\omega(-G\omega^2 + I) + HK\omega,\\
\tilde{d} &= -A\omega^2(-D\omega^2 + F) + C(-D\omega^2 + F) - E\omega^4 + BE\omega^2 - K(-G\omega^2 + I) - HJ\omega^2,\\
\tilde{e} &= C^2 + F^2 - I^2 - K^2.
\end{aligned}$$

Similar to Case II, (3.13) has a finite number of positive roots $\omega_1, \omega_2, \ldots, \omega_k$ when

$$(C + F)^2 - (I + K)^2 < 0. \tag{3.14}$$

Then, we have calculated the value of τ_2 as $\tilde{\tau}^j_{2_p}$ given by

$$\tilde{\tau}^j_{2_p} = \frac{1}{\omega_p}\sin^{-1}\left(\frac{M_pQ_p + N_pS_p}{M_p^2 + N_p^2}\right) + \frac{2j\pi}{\omega_p}, \tag{3.15}$$

for $p = 1, 2, \ldots, k$; $j = 0, 1, 2 \ldots$, where

$$\begin{aligned}
M_P &= (-G\omega_p^2 + I) + J\omega_p\sin(\omega_p\tilde{\tau}_1) + K\cos(\omega_p\tilde{\tau}_1),\\
N_p &= -H\omega_p - J\omega_p\cos(\omega_p\tilde{\tau}_1) + K\sin(\omega_p\tilde{\tau}_1),\\
Q_p &= -\omega_p^3 + B\omega_p + E\omega_p\cos(\omega_p\tilde{\tau}_1) - (-D\omega_p^2 + F)\sin(\omega_p\tilde{\tau}_1),\\
S_p &= -\omega_p^2A + C + (-D\omega_p^2 + F)\cos(\omega_p\tilde{\tau}_1) + E\omega_p\sin(\omega_p\tilde{\tau}_1).
\end{aligned}$$

Let $\tilde{\tau}^j_{2_0} = \min\{\tilde{\tau}^j_{2_p} \mid p = 1, 2, \ldots, k; j = 0, 1, 2, \ldots\}$, and by assuming that

$$\frac{d}{d\tau_2}\mathrm{Re}(\lambda)\Big|_{\lambda = i\omega_p} \neq 0,$$

we have the following theorem.

THEOREM 3.2. *Suppose that the parameters in model* (2.3) *are such that the conditions* (3.4)–(3.6), (3.11) *and* (3.14) *hold for* $\tau_1 \in (0, \tau_{1_0})$. *Then the coexistence equilibrium* $E^*(x^*, y^*, z^*)$ *is locally asymptotically stable when* $\tau_2 \in (0, \tilde{\tau}^j_{2_0})$ *and it is unstable when* $\tau_2 > \tilde{\tau}^j_{2_0}$. *Moreover, Hopf-bifurcation occurs when* $\tau_2 = \tilde{\tau}^j_{2_0}$.

https://doi.org/10.1017/S144618111700044X Published online by Cambridge University Press

Case IV: $\tau_1 = 0$ and $\tau_2 \neq 0$.
Similar to Case II, we calculate the critical value of τ_2 in this case. For every fixed $\omega_l, l = 1, 2, \ldots, k$, there exist a sequence $\{\tau_{2_l}^j | j = 0, 1, 2, \ldots\}$, where

$$\tau_{2_l}^j = \frac{1}{\omega_l} \cos^{-1}\left[\frac{\Phi}{\Psi}\right] + \frac{2j\pi}{\omega_l} \tag{3.16}$$

such that $l = 1, 2, \ldots, k$; $j = 0, 1, 2 \ldots$, where

$$\Phi = \omega_l^4(H + J) - \omega_l^2(B + E)(H + J) + (G\omega_l^2 - I - K)(-\omega_l^2(A + D) + (C + F)),$$
$$\Psi = (-G\omega_l^2 + I + K)^2 + \omega_l^2(H + J)^2,$$

and if condition (3.14) holds, then $\omega_l, l = 1, 2, \ldots, k$ are the finite positive roots of the equation

$$\omega^6 + \check{a}\omega^4 + \check{b}\omega^2 + \check{c} = 0, \tag{3.17}$$

where,

$$\check{a} = (A + D)^2 - 2(B + E) - G^2,$$
$$\check{b} = (B + E)^2 - 2(A + D)(C + F) + 2G(I + K) - (H + J)^2,$$
$$\check{c} = (C + F)^2 - (I + K)^2.$$

Let $\tau_{2_0} = \min\{\tau_{2_l}^j \mid l = 1, 2, \ldots, k; j = 0, 1, 2, \ldots\}$. We have also obtained

$$\left\{\frac{d}{d\tau_2} \mathrm{Re}(\lambda)\right\}_{\tau_2 = \tau_{2_0}} = \frac{\eta_3\rho_3 - \eta_4\rho_4}{\hat{\Omega}} > 0$$

provided that $\eta_3\rho_3 - \eta_4\rho_4 > 0$, where

$$\hat{\Omega} = (\omega_l(I + K) - \omega_l^3 G)^2 + \omega_l^4(H + J)^2,$$
$$\eta_3 = (-3\omega_l^2 + B + E)\sin\omega_l\tau_2 + 2\omega_l(A + D)\cos\omega_l\tau_2 + 2\omega_l G,$$
$$\rho_1 = \omega_l(I + K) - \omega_l^3 G,$$
$$\eta_2 = (-3\omega_l^2 + B + E)\cos\omega_l\tau_2 - 2\omega_l(A + D)\sin\omega_l\tau_2 + (H + J),$$
$$\rho_2 = \omega_l^2(H + J).$$

Then, by the general Hopf-bifurcation theorem, we have the following result on the stability and bifurcation of the system (2.3).

THEOREM 3.3. *Assume that the conditions* (3.4)–(3.6) *and* (3.14) *hold. Then the equilibrium* $E^*(x^*, y^*, z^*)$ *is locally asymptotically stable for* $\tau_2 < \tau_{2_0}$ *and unstable for* $\tau_2 > \tau_{2_0}$. *Furthermore, the system* (2.3) *undergoes a Hopf-bifurcation at* $E^*(x^*, y^*, z^*)$ *when* $\tau_2 = \tau_{2_0}$.

Case V: $\tau_2 \in (0, \tau_{2_0}), \tau_1 \neq 0$.
Similar to Case III, we have calculated the critical value of τ_1 for a fixed value of τ_2 and stated the results as follows.

THEOREM 3.4. *Suppose that the parameters in model system* (2.3) *are such that conditions* (3.4)–(3.6), (3.14) *and* (3.11) *hold for* $\tau_2 \in (0, \tau_{2_0})$. *Then the coexistence equilibrium* $E^*(x^*, y^*, z^*)$ *is locally asymptotically stable when* $\tau_1 \in (0, \tilde{\tau}_{1_0}^j)$, *and it is*

https://doi.org/10.1017/S144618111700044X Published online by Cambridge University Press

unstable when $\tau_1 > \tilde{\tau}^j_{1_0}$. *Moreover, Hopf-bifurcation occurs when* $\tau_1 = \tilde{\tau}^j_{1_0}$, *such that* $\tilde{\tau}^j_{1_0} = \min\{\tilde{\tau}^j_{1_s} \mid s = 1, 2, \ldots, k;\ j = 0, 1, 2, \ldots\}$, *where*

$$\tilde{\tau}^j_{1_s} = \frac{1}{\omega_s} \sin^{-1} \frac{V_s T_s + W_s U_s}{V_s^2 + W_s^2} + \frac{2j\pi}{\omega_s}, \tag{3.18}$$

and

$$\begin{aligned}
V_s &= (-D\omega_s^2 + F) + J\omega_s \sin \omega_s \tau_{2_0} + K \cos \omega_s \tau_{2_0},\\
W_s &= -E\omega_s - J\omega_s \cos \omega_s \tau_{2_0} + K \sin \omega_s \tau_{2_0},\\
T_s &= -\omega_s^3 + B\omega_s + H\omega_s \cos \omega_s \tau_{2_0} - (-G\omega_s^2 + I) \sin \omega_s \tau_{2_0},\\
U_s &= -\omega_s^2 A + C + (-G\omega_s^2 + I) \cos \omega_s \tau_{2_0} + H\omega_s \sin \omega_s \tau_{2_0}.
\end{aligned}$$

3.1. Global stability analysis We now establish the following result.

THEOREM 3.5. *If* $\min\{\gamma_1, \gamma_2, \gamma_3\} > 0$, *with*

$$\begin{aligned}
\gamma_1 &= -\frac{y^*}{m_1(x^* + \omega_4)} + \frac{\omega_6 y^*}{m_2(x^* + \omega_7)}\left(-1 + \frac{\omega_6 M_2 \tau_1}{m_2}\right),\\
\gamma_2 &= \frac{1}{M_1} + \frac{\omega_6 x^*}{(x^* + \omega_7)}\left(\frac{1}{M_2} - \frac{\omega_6 M_2 \tau_1}{m_2^2}\right) - \frac{\omega_6}{m_2}\left(1 - \frac{\omega_6 M_2 \tau_1}{m_2}\right)\\
&\quad - \frac{z^*}{m_2 \Omega}\left(1 - \omega_6 M_2 \tau_1\right) - \frac{\omega_{12} z^*}{m_3 \Omega}\left(1 - \frac{\omega_{12} M_3 (y^* + \omega_{10})\tau_2}{m_3 \Omega}\right),\\
\gamma_3 &= \frac{y^* + \omega_{10}}{m_2 \Omega}\left(1 - \omega_6 M_2 \tau_1\right) + \frac{\omega_{12} y^*}{M_3 \Omega} - \frac{\omega_{12}(y^* + \omega_{10})}{m_3 \Omega}\\
&\quad \times \left(1 + \frac{\omega_{12} M_3 y^* \tau_2}{m_3 \Omega} - \frac{\omega_{12} M_3 (y^* + \omega_{10})\tau_2}{m_3 \Omega}\right),
\end{aligned}$$

where $\Omega = (y^* + (\omega_8 + \omega_9 y^*)z^* + \omega_{10})$, $m_1 < x(t) < M_1$, $m_2 < y(t) < M_2$ *and* $m_3 < z(t) < M_3$ *for* $t > 0$, *then the interior equilibrium* E^* *of the model system* (2.3) *is globally asymptotically stable.*

PROOF. Proof is given in Appendix A.2 (Supplementary material). □

4. Properties of periodic solutions

In Section 3, we have obtained sufficient conditions for system (2.3) to undergo Hopf-bifurcation for different combinations of τ_1 and τ_2. In this section, we study the properties of solutions of the bifurcating equilibrium point. These properties are studied with respect to τ_1 for fixed $\tau_2 \in (0, \tau_{2_0})$. The technique we use is based on the normal form method and the centre manifold theory presented by Hassard et al. [13]. Throughout this section, we assume that the system undergoes Hopf-bifurcation at $\tau_1 = \tilde{\tau}_{1_0}$ and $\tau_2 \in (0, \tau_{2_0})$ at $E^*(x^*, y^*, z^*)$. Let $\tau_1 = \tilde{\tau}_{1_0} + \mu$, $\mu \in R$ so that Hopf-bifurcation occurs at $\mu = 0$. Without loss of generality, it is assumed that $\tau_2^* < \tilde{\tau}_{1_0}$ where $\tau_2^* \in (0, \tau_{2_0})$. Let $x_1(t) = x(t) - x^*$, $y_1(t) = y(t) - y^*$, $z_1(t) = z(t) - z^*$, and denote

https://doi.org/10.1017/S144618111700044X Published online by Cambridge University Press

$x_1(t), y_1(t), z_1(t)$ by $x(t), y(t), z(t)$, respectively. We normalize the delay with the scaling $t \to (t/\tau_1)$, so that system (2.3) may be rewritten as

$$\dot{u}(t) = \tau_1 M_1 u(t) + \tau_1 M_2 u\left(t - \frac{\tau_2^*}{\tilde{\tau}_{1_0}}\right) + \tau_1 M_3 u(t-1) + \tau_1 f(x, y, z), \tag{4.1}$$

where $u(t) = (x(t), y(t), z(t))^T$,

$$M_1 = \begin{pmatrix} a_{11} & a_{12} & 0 \\ 0 & a_{22} & a_{23} \\ 0 & 0 & a_{33} \end{pmatrix}, \quad M_2 = \begin{pmatrix} 0 & 0 & 0 \\ 0 & 0 & 0 \\ 0 & c_{23} & c_{33} \end{pmatrix},$$

$$M_3 = \begin{pmatrix} 0 & 0 & 0 \\ b_{21} & b_{22} & 0 \\ 0 & 0 & 0 \end{pmatrix}, \quad f = (f_1, f_2, f_3)^T.$$

The nonlinear terms

$$\begin{aligned} f_1 &= -x^2(t) + e_1 x^2(t) + e_2 x(t)y(t) + E^* y^2(t) + e_4 x^3(t) + e_5 x^2(t)y(t) + e_6 x(t)y^2(t) \\ &\quad + e_7 y^3(t) + h.o.t, \quad \text{(higher order terms)} \\ f_2 &= p_1 x^2(t-1) + p_2 x(t-1)y(t-1) + p_3 y^2(t-1) + p_4 x^3(t-1) + p_5 x^2(t-1)y(t-1) \\ &\quad + p_6 x(t-1)y^2(t-1) + p_7 y^3(t-1) + q_1 y^2(t) + q_2 y(t)z(t) + q_3 z^2(t) + q_4 y^3(t) \\ &\quad + q_5 y^2(t)z(t) + q_6 y(t)z^2(t) + q_7 z^3(t) + h.o.t, \\ f_3 &= r_1 y^2\left(t - \frac{\tau_2^*}{\tilde{\tau}_{1_0}}\right) + r_2 y\left(t - \frac{\tau_2^*}{\tilde{\tau}_{1_0}}\right) z\left(t - \frac{\tau_2^*}{\tilde{\tau}_{1_0}}\right) + r_3 z^2\left(t - \frac{\tau_2^*}{\tilde{\tau}_{1_0}}\right) + r_4 y^3\left(t - \frac{\tau_2^*}{\tilde{\tau}_{1_0}}\right) \\ &\quad + r_5 y^2\left(t - \frac{\tau_2^*}{\tilde{\tau}_{1_0}}\right) z\left(t - \frac{\tau_2^*}{\tilde{\tau}_{1_0}}\right) + r_6 y\left(t - \frac{\tau_2^*}{\tilde{\tau}_{1_0}}\right) z^2\left(t - \frac{\tau_2^*}{\tilde{\tau}_{1_0}}\right) + r_7 z^3\left(t - \frac{\tau_2^*}{\tilde{\tau}_{1_0}}\right) + h.o.t. \end{aligned}$$

where $e_i, p_i, q_i, r_i; (i = 1, 2, \ldots, 7)$ are given in Appendix A.3 (Supplementary material). For $\phi = (\phi_1, \phi_2, \phi_3)^T \in C([-1, 0], R^3)$, define

$$L_\mu \phi = (\tau_1 + \mu)\left(M_1 \phi(0) + M_2 \phi\left(-\frac{\tau_2^*}{\tilde{\tau}_{1_0}}\right) + M_3 \phi(-1)\right).$$

By the Riesz representation theorem [13], there exists a function $\eta(\theta, \mu)$ whose components are of bounded variation for $\theta \in [-1, 0]$, such that

$$L_\mu \phi = \int_{-1}^{0} \phi(\theta)\, d\eta(\theta, \mu) \quad \text{for } \phi \in C.$$

In fact, choosing

$$\eta(\theta, \mu) = \begin{cases} (\tilde{\tau}_{1_0} + \mu)(M_1 + M_2 + M_3), & \theta = 0, \\ (\tilde{\tau}_{1_0} + \mu)(M_2 + M_3), & \theta \in \left[-\dfrac{\tau_2^*}{\tilde{\tau}_{1_0}}, 0\right), \\ (\tilde{\tau}_{1_0} + \mu)M_3, & \theta \in \left[-1, \dfrac{\tau_2^*}{\tilde{\tau}_{1_0}}\right), \\ 0, & \theta = -1, \end{cases}$$

https://doi.org/10.1017/S144618111700044X Published online by Cambridge University Press

for $\phi \in C^1([-1,0],R^3)$, we define

$$A(\mu)\phi = \begin{cases} \dfrac{d\phi(\theta)}{d\theta}, & \theta \in [-1,0), \\ \displaystyle\int_{-1}^{0} \phi(\xi)\, d\eta(\xi,\mu), & \theta = 0, \end{cases}$$

and

$$R(\mu)\phi = \begin{cases} 0, & \theta \in [-1,0), \\ h(\mu,\theta), & \theta = 0, \end{cases}$$

where

$$\begin{aligned} h(\mu,\phi) &= (\tilde{\tau}_{1_0}+\mu)(h_1,h_2,h_3)^T, \quad \phi = (\phi_1,\phi_2,\phi_3)^T \in C([-1,0],R^3) \\ f_1 &= -\phi_1^2(0) + e_1\phi_1^2(0) + e_2\phi_1(0)\phi_2(0) + E^*\phi_2^2(0) + e_4\phi_1^3(0) + e_5\phi_1^2(0)\phi_2(0) \\ &\quad + e_6\phi_1(0)\phi_2^2(0) + e_7\phi_2^3(0) + \cdots, \\ f_2 &= p_1\phi_1^2(-1) + p_2\phi_1(-1)\phi_2(-1) + p_3\phi_2^2(-1) + p_4\phi_1^3(-1) + p_5\phi_1^2(-1)\phi_2(-1) \\ &\quad + p_6\phi_1(-1)\phi_2^2(-1) + p_7\phi_2^3(-1) + q_1\phi_2^2(0) + q_2\phi_2(0)\phi_3(0) + q_3\phi_3^2(0) \\ &\quad + q_4\phi_2^3(0) + q_5\phi_2^2(0)\phi_3(0) + q_6\phi_2(0)\phi_3^2(0) + q_7\phi_3^3(0) + \cdots, \\ f_3 &= r_1\phi_2^2\Big(-\frac{\tau_2^*}{\tilde{\tau}_{1_0}}\Big) + r_2\phi_2\Big(-\frac{\tau_2^*}{\tilde{\tau}_{1_0}}\Big)\phi_3\Big(-\frac{\tau_2^*}{\tilde{\tau}_{1_0}}\Big) + r_3\phi_3^2\Big(-\frac{\tau_2^*}{\tilde{\tau}_{1_0}}\Big) + r_4\phi_2^3\Big(-\frac{\tau_2^*}{\tilde{\tau}_{1_0}}\Big) \\ &\quad + r_5\phi_2^2\Big(-\frac{\tau_2^*}{\tilde{\tau}_{1_0}}\Big)\phi_3\Big(-\frac{\tau_2^*}{\tilde{\tau}_{1_0}}\Big) + r_6\phi_2\Big(-\frac{\tau_2^*}{\tilde{\tau}_{1_0}}\Big)\phi_3^2\Big(-\frac{\tau_2^*}{\tilde{\tau}_{1_0}}\Big) + r_7\phi_3^3\Big(-\frac{\tau_2^*}{\tilde{\tau}_{1_0}}\Big) + \cdots. \end{aligned}$$

The system (2.3) may be rewritten in the following form

$$\dot{u}_t = A(\mu)u_t + R(\mu)u_t, \tag{4.2}$$

where $u_t(\theta) = u(t+\theta)$, $u(t) = (x(t),y(t),z(t))^T$ for $\theta \in [-1,0]$. For $\psi \in C([0,1],(R^3)^*)$, define

$$A^*\psi(s) = \begin{cases} -\dfrac{d\psi(s)}{ds}, & s \in (0,1], \\ \displaystyle\int_{-1}^{0} \psi(-\xi)\, d\eta^T(\xi,0), & s = 0, \end{cases}$$

and a bilinear inner product

$$\langle \psi,\phi\rangle = \bar{\psi}(0)\cdot\phi(0) - \int_{\theta=-1}^{0}\int_{\xi=0}^{\theta} \bar{\psi}(\xi-\theta)\, d\eta(\theta)\phi(\xi)\, d\xi,$$

where $\eta(\theta) = \eta(\theta,0)$. Then $A(0)$ (here onwards we denote $A(0)$ by A) and A^* are adjoint operators. Since $\pm i\omega_0\tilde{\tau}_{1_0}$ are the eigenvalues of A, they are also the eigenvalues of A^*. We need to compute eigenvectors of A and A^* corresponding to $i\omega_0\tilde{\tau}_{1_0}$ and $-i\omega_0\tilde{\tau}_{1_0}$, respectively. By direct computation, it is not difficult to obtain the vector $q(\theta) = (1,a_1,a_2)^T e^{i\omega_0\tilde{\tau}_{1_0}\theta}$, $(\theta \in [-1,0])$ and $q^*(s) = M(1,a_1^*,a_2^*)e^{i\omega_0\tilde{\tau}_{1_0}s}$, $(s \in [0,1])$ where a_1, a_2, a_1^*, a_2^* and M are given in Appendix A.4 (Supplementary material).

https://doi.org/10.1017/S144618111700044X Published online by Cambridge University Press

Furthermore, $\langle q^*(s), q(\theta)\rangle = 1$ and $\langle q^*(s), \bar{q}(\theta)\rangle = 0$. Proceeding in the same manner as in Hassard et al. [13], we compute the coordinates to describe the centre manifold C_0 at $\mu = 0$. Let x_t be the solution of equation (4.1) when $\mu = 0$. Define

$$z(t) = \langle q^*, u_t\rangle, \quad W(t,\theta) = u_t(\theta) - 2\,\mathrm{Re}\{z(t)q(\theta)\}. \tag{4.3}$$

On the center manifold C_0,

$$W(t,\theta) = W(z,\bar{z},\theta) = W_{20}(\theta)\frac{z^2}{2} + W_{11}(\theta)z\bar{z} + W_{02}(\theta)\frac{\bar{z}^2}{2} + \cdots,$$

and z, $\bar{z}$ are local coordinates for centre manifold C_0 in the direction of q^* and $\bar{q}^*$, respectively. We now consider only the real solution $x_t \in C_0$ of equation (4.1), which gives

$$\dot{z} = i\omega_0\tilde{\tau}_{1_0}z + \bar{q}^* \cdot f(0, W(z,\bar{z},0) + 2\,\mathrm{Re}\{zq(0)\}) = i\omega_0\tilde{\tau}_{1_0}z + g(z,\bar{z}),$$

where

$$g(z,\bar{z}) = \bar{q}^*(0)f_0(z,\bar{z}) = g_{20}\frac{z^2}{2} + g_{11}z\bar{z} + g_{02}\frac{\bar{z}^2}{2} + g_{21}\frac{z^2\bar{z}}{2} + \cdots. \tag{4.4}$$

Hence, we have to obtain the expressions for $g(z,\bar{z})$ (Appendix A.5 in Supplementary material) and for $g_{20}, g_{11}, g_{02}, g_{21}$ (Appendix A.5 in Supplementary material).

In order to compute g_{21}, we need to compute $W_{20}(i)(\theta), W_{11}(i)(\theta), (i = 1, 2)$. From equations (4.2) and (4.3),

$$\begin{aligned}\dot{W} &= \dot{x}_t - \dot{z}q - \dot{\bar{z}}\bar{q}\\ &= \begin{cases} AW - 2\,\mathrm{Re}\{\bar{q}^*(0)f_0q(\theta)\}, & \theta \in [-1,0),\\ AW - 2\,\mathrm{Re}\{\bar{q}^*(0)f_0q(\theta)\} + f_0, & \theta = 0,\end{cases}\\ &= AW + H(z,\bar{z},\theta),\end{aligned} \tag{4.5}$$

with

$$H(z,\bar{z},\theta) = H_{20}(\theta)\frac{z^2}{2} + H_{11}(\theta)z\bar{z} + H_{02}(\theta)\frac{z^2}{2} + \cdots. \tag{4.6}$$

Following Hassard et al. [13], from equations (4.5) and (4.6), we get

$$H_{20}(0) = -g_{20}q(0) - \bar{g}_{02}\bar{q}(0) + 2\tilde{\tau}_{1_0}(H_1, H_2, H_3)^T,$$

and

$$H_{11}(0) = -g_{11}q(0) - \bar{g}_{11}\bar{q}(0) + 2\tilde{\tau}_{1_0}(P_1, P_2, P_3)^T,$$

where $H_1, H_2, H_3, P_1, P_2, P_3$ are given in Appendix A.6 (Supplementary material). Also,

$$\left(i\omega_0\tilde{\tau}_{1_0}I - \int_{-1}^{0} e^{i\omega_0\tilde{\tau}_{1_0}\theta}\,d\eta(\theta)\right)q(0) = 0,$$

and noticing that

$$\left(-i\omega_0\tilde{\tau}_{1_0}I - \int_{-1}^{0} e^{-i\omega_0\tilde{\tau}_{1_0}\theta}\,d\eta(\theta)\right)\bar{q}(0) = 0,$$

we obtain

$$\left(2i\omega_0\tilde{\tau}_{1_0}I - \int_{-1}^{0} e^{2i\omega_0\tilde{\tau}_{1_0}\theta}\,d\eta(\theta)\right)E_1 = 2\tilde{\tau}_{1_0}(H_1, H_2, H_3)^T.$$

https://doi.org/10.1017/S144618111700044X Published online by Cambridge University Press

This leads to

$$\begin{pmatrix} 2i\omega_0 - a_{11} & -a_{12} & 0 \\ -b_{21}e^{-2i\omega_0\tilde{\tau}_{1_0}} & 2i\omega_0 - a_{22} - b_{22}e^{-2i\omega_0\tilde{\tau}_{1_0}} & -a_{23} \\ 0 & -c_{32}e^{-2i\omega_0\tau_2^*} & 2i\omega_0 - a_{33} - c_{33}e^{-2i\omega_0\tau_2^*} \end{pmatrix} E_1 = 2\begin{pmatrix} H_1 \\ H_2 \\ H_3 \end{pmatrix}.$$

Solving this system for E_1, we obtain

$$E_1^{(1)} = \frac{2}{\tilde{A}}\begin{vmatrix} H_1 & -a_{12} & 0 \\ H_2 & 2i\omega_0 - a_{22} - b_{22}e^{-2i\omega_0\tilde{\tau}_{1_0}} & -a_{23} \\ H_3 & -c_{32}e^{-2i\omega_0\tau_2^*} & 2i\omega_0 - a_{33} - c_{33}e^{-2i\omega_0\tau_2^*} \end{vmatrix},$$

$$E_1^{(2)} = \frac{2}{\tilde{A}}\begin{vmatrix} 2i\omega_0 - a_{11} & H_1 & 0 \\ -b_{21}e^{-2i\omega_0\tilde{\tau}_{1_0}} & H_2 & -a_{23} \\ 0 & H_3 & 2i\omega_0 - a_{33} - c_{33}e^{-2i\omega_0\tau_2^*} \end{vmatrix},$$

$$E_1^{(3)} = \frac{2}{\tilde{A}}\begin{vmatrix} 2i\omega_0 - a_{11} & -a_{12} & H_1 \\ -b_{21}e^{-2i\omega_0\tilde{\tau}_{1_0}} & 2i\omega_0 - a_{22} - b_{22}e^{-2i\omega_0\tilde{\tau}_{1_0}} & H_2 \\ 0 & -c_{32}e^{-2i\omega_0\tau_2^*} & H_3 \end{vmatrix},$$

where

$$\tilde{A} = \begin{vmatrix} 2i\omega_0 - a_{11} & -a_{12} & 0 \\ -b_{21}e^{-2i\omega_0\tilde{\tau}_{1_0}} & 2i\omega_0 - a_{22} - b_{22}e^{-2i\omega_0\tilde{\tau}_{1_0}} & -a_{23} \\ 0 & -c_{32}e^{-2i\omega_0\tau_2^*} & 2i\omega_0 - a_{33} - c_{33}e^{-2i\omega_0\tau_2^*} \end{vmatrix}.$$

Similarly, we get

$$\begin{pmatrix} -a_{11} & -a_{12} & 0 \\ -b_{21} & -a_{22} - b_{22} & -a_{23} \\ 0 & -c_{32} & -a_{33} - c_{33} \end{pmatrix} E_2 = 2\begin{pmatrix} P_1 \\ P_2 \\ P_3 \end{pmatrix},$$

and hence

$$E_2^{(1)} = \frac{2}{\tilde{B}}\begin{vmatrix} P_1 & -a_{12} & 0 \\ P_2 & -a_{22} - b_{22} & -a_{23} \\ P_3 & -c_{32} & -a_{33} - c_{33} \end{vmatrix},$$

$$E_2^{(2)} = \frac{2}{\tilde{B}}\begin{vmatrix} -a_{11} & P_1 & 0 \\ -b_{21} & P_2 & -a_{23} \\ 0 & P_3 & -a_{33} - c_{33} \end{vmatrix}$$

$$E_2^{(3)} = \frac{2}{\tilde{B}}\begin{vmatrix} -a_{11} & -a_{12} & P_1 \\ -b_{21} & -a_{22} - b_{22} & P_2 \\ 0 & -c_{32} & P_3 \end{vmatrix},$$

https://doi.org/10.1017/S144618111700044X Published online by Cambridge University Press

where

$$\tilde{B} = \begin{vmatrix} -a_{11} & -a_{12} & 0 \\ -b_{21} & -a_{22} - b_{22} & -a_{23} \\ 0 & -c_{32} & -a_{33} - c_{33} \end{vmatrix}.$$

Thus, we can determine $W_{20}(\theta)$ and $W_{11}(\theta)$. Furthermore, g_{21} in equation (4.4) may be expressed by the model parameters and delay. Thus, we compute the following values

$$\begin{aligned} c_1(0) &= \frac{i}{2\omega_0\tilde{\tau}_{1_0}}\left(g_{20}g_{11} - 2|g_{11}|^2 - \frac{|g_{02}|^2}{3}\right) + \frac{g_{21}}{2}, \\ \mu_2 &= -\frac{\mathrm{Re}\{c_1(0)\}}{\mathrm{Re}\{\lambda'(\tilde{\tau}_{1_0})\}}, \\ \beta_2 &= 2\,\mathrm{Re}\{c_1(0)\}, \\ T_2 &= -\frac{\mathrm{Im}\{c_1(0)\} + \mu_2\,\mathrm{Im}\{\lambda'(\tilde{\tau}_{1_0})\}}{\omega_0\tau_0}, \end{aligned} \tag{4.7}$$

which determine the properties of the bifurcating periodic solutions in the centre manifold at the critical value $\tilde{\tau}_{1_0}$. Now we state the results in the following theorem.

THEOREM 4.1. *For the expressions given in equation (4.7), the following results hold.*

(1) *The sign of μ_2 determines the direction of the Hopf-bifurcation. If $\mu_2 > 0$, then the Hopf-bifurcation is supercritical, and the bifurcating periodic solutions exist for $\tau > \tilde{\tau}_{1_0}$. If $\mu_2 < 0$, then the Hopf-bifurcation is subcritical and the bifurcating periodic solutions exist for $\tau < \tilde{\tau}_{1_0}$.*
(2) *The parameter β_2 determines the stability of the bifurcating periodic solutions. The bifurcating periodic solutions are stable if $\beta_2 < 0$ and are unstable if $\beta_2 > 0$.*
(3) *Also, T_2 determines the period of the bifurcating periodic solutions. The period of the bifurcating periodic solutions increases if $T_2 > 0$ and decreases if $T_2 < 0$.*

5. Numerical simulations

We perform numerical computations to realize various dynamics of the coexistence equilibrium point $E^*(x^*, y^*, z^*)$ for the model systems (2.3), (5.1) and (5.2), respectively. For this purpose, we use standard packages (ode45 and dde23) of MATLAB 7.6.0 (R2008a). First we consider the following fixed parameter values

$$\begin{aligned} \mathrm{Set}_1 : \omega_4 = 0.35, \quad \omega_5 = 0.152, \quad \omega_6 = 0.42, \quad \omega_7 = 0.65, \quad \omega_8 = 0.01, \\ \omega_9 = 0.21, \quad \omega_{10} = 0.48, \quad \omega_{11} = 0.015, \quad \omega_{12} = 0.05. \end{aligned}$$

https://doi.org/10.1017/S144618111700044X Published online by Cambridge University Press

Table 1. Stability results of system (2.3) with parameter Set$_1$.

Case	Condition	Critical value	Delay value	Status	Figure 2
I	$\mu_1 = 0.673 > 0$, $\mu_2 = 7.5327 \times 10^{-4} > 0$, $\Delta = 6.2566 \times 10^{-5} > 0$	NA	NA	Stable	Case I
II	$\Sigma = 3.9987 \times 10^{-7} > 0$, with condition of Case I	NA	$\tau_1 = 0.1, \tau_2 = 0$	Stable	Case II(i)
			$\tau_1 = 1.5, \tau_2 = 0$	Stable	Case II(ii)
III	$\Sigma = 3.9987 \times 10^{-7} > 0$, $\Psi = -3.3061 \times 10^{-7} < 0$, with condition of Case I	NA	$\tau_1 = 0.1, \tau_2 = 0.5$	Stable	Case III(i)
			$\tau_1 = 0.1, \tau_2 = 3$	Stable	Case III(ii)
IV	$\Psi = -3.3061 \times 10^{-7} < 0$, with condition of Case I	$\omega_0 = 0.0291$, $\tau_{2_0} = 1.6079$	$\tau_1 = 0, \tau_2 = 0.6$	Stable	Case IV(i)
			$\tau_1 = 0, \tau_2 = 11.7$	Unstable	Case IV(ii)
V	$\Sigma = 3.9987 \times 10^{-7} > 0$, $\Psi = -3.3061 \times 10^{-7} < 0$, with condition of Case I	NA	$\tau_1 = 0.1, \tau_2 = 0.6$	Stable	Case V(i)
			$\tau_1 = 5, \tau_2 = 0.6$	Stable	Case V(ii)

By using this parameter set, the co-existence abundance is $x^* = 0.8233, y^* = 0.2073$ and $z^* = 0.0571$. First we observe the two-dimensional bifurcation scenario of system (2.3) in the $\tau_1\tau_2$-plane (Figure 1(a)). On the red line on the τ_2-axis, the system (2.3) is unstable, while in the rest of the plane the system is stable. Also, when τ_2 crosses the critical value $\tau_{2_0} = 1.6079$, the system exhibits Hopf-bifurcation. These two different characteristic dynamical phenomena are presented numerically in this section. We show five different numerical examples corresponding to five analytical results (Cases (I)–(V)) (See Table 1).

(i) For Case I, first we consider the system (2.3) when $\tau_1 = \tau_2 = 0$. Then $\mu_1 = 0.673 > 0, \mu_2 = 7.5327 \times 10^{-4} > 0$ and $\Delta = 6.2566 \times 10^{-5} > 0$. In this case, the system is asymptotically stable (Figure 2 (Case I)).

(ii) For Case II, $(C + I)^2 - (F + K)^2 (= \Sigma) = 3.9987 \times 10^{-7} > 0$, hence the parameter set does not satisfy the criteria of conditional stability. In this case, the system is asymptotically stable for all $\tau_1 \geq 0$ (Figure 2 (Case II(i)): $\tau_1 = 0.1$ and Figure 2 (Case II(ii)): $\tau_1 = 1.5$).

(iii) For Case III, $(C + I)^2 - (F + K)^2 = 3.9987 \times 10^{-7} > 0, (C + F)^2 - (I + K)^2 (= \Psi) = -3.3061 \times 10^{-7} < 0$, so the parameter set does not satisfy the criteria of conditional stability. In this case, the system is asymptotically stable for all $\tau_1, \tau_2 \geq 0$ (Figure 2 (Case III(i)): $\tau_1 = 0.1, \tau_2 = 0.5$ and Figure 2 (Case III(ii)): $\tau_1 = 0.1, \tau_2 = 3$).

(iv) For Case IV, we see that $(C + F)^2 - (I + K)^2 = -3.3061 \times 10^{-7} < 0$, the parameter set satisfies the conditional stability criteria. Here, $\omega_0 = 0.0291$ and $\tau_{2_0} = 1.6079$. In this case, the system is asymptotically stable for $0 < \tau_2 = 0.6 <$

https://doi.org/10.1017/S144618111700044X Published online by Cambridge University Press

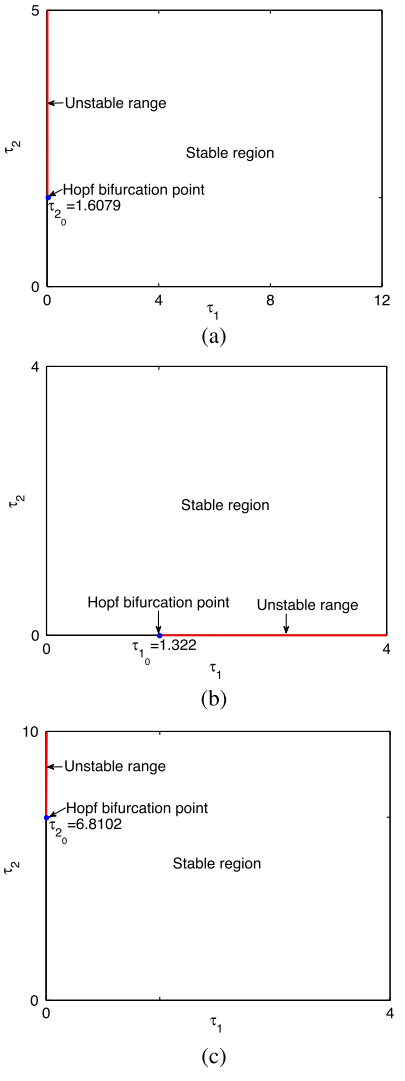

FIGURE 1. Stability regions of system (2.3) (a), system (5.1) (b) and system (5.2) (c) in the $\tau_1\tau_2$-plane where the systems shows stable and unstable dynamics in the 'stable region' and 'unstable range' (red line), respectively. Hopf-bifurcation occurs when (a) τ_2 crosses the critical value $\tau_{2_0} = 1.6079$, (b) τ_1 crosses the critical value $\tau_{1_0} = 1.322$ and (c) τ_2 crosses the critical value $\tau_{2_0} = 6.8102$. Rather than Case IV, other cases of system (2.3) (a), system (5.1) (b) and system (5.2) (c) are absolutely stable by the choice of different combinations of τ_1 and τ_2. Parameters are as in the text (colour available online).

$\tau_{2_0} = 1.6079$ (Figure 2 (Case IV(i))) and unstable for $\tau_2 = 11.7 > \tau_{2_0} = 1.6079$ (Figure 2 (Case IV(ii))). The system experiences Hopf-bifurcation when the delay parameter τ_2 crosses its critical value $\tau_{2_0} = 1.6079$.

https://doi.org/10.1017/S144618111700044X Published online by Cambridge University Press

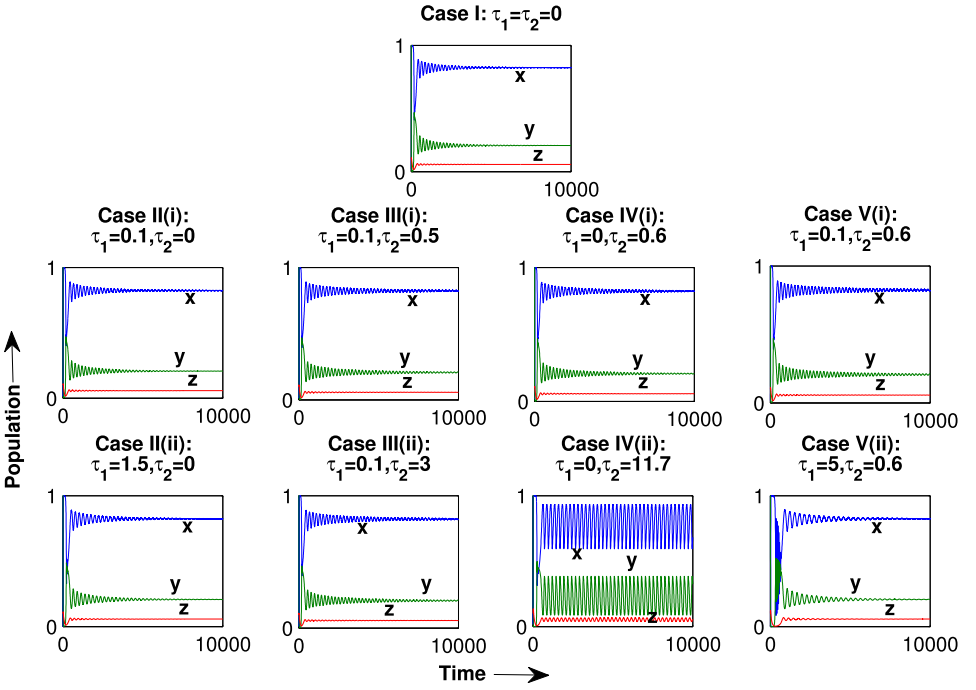

FIGURE 2. Time evolution of system (2.3) with parameter Set$_1$. For Case I, when $\tau_1 = \tau_2 = 0$, the positive interior equilibrium $E_3(0.8233, 0.2073, 0.0571)$ is locally asymptotically stable. For Case II ($\tau_2 = 0$), system remains stable for all $\tau_1 \geq 0$. Similarly for Case III, system is stable for all $\tau_2 \geq 0$ by choosing $\tau_1 = 0.1$. For Case IV ($\tau_1 = 0$), the system remains stable at $\tau_2 = 0.6 < \tau_{2_0} = 1.6079$ and it shows stable periodic solution at $\tau_2 = 11.7 > \tau_{2_0} = 1.6079$. Again for Case V, the system is stable for all $\tau_1 \geq 0$ by choosing $\tau_2 = 0.6$. Parameters are as in the text.

(v) For Case V, it turns out that $(C + I)^2 - (F + K)^2 = 3.9987 \times 10^{-7} > 0, (C + F)^2 - (I + K)^2 = -3.3061 \times 10^{-7} < 0$, so the parameter set does not satisfy the conditional stability criteria. In this case, the system is asymptotically stable for all $\tau_1 \geq 0$ while $\tau_2 \in [0, \tau_{2_0})$ (Figure 2 (Case V(i)): $\tau_1 = 0.1, \tau_2 = 0.6$ and Figure 2 (Case V(ii)): $\tau_1 = 5, \tau_2 = 0.6$).

We can verify the previous results by following the bifurcation diagram (Figure 3(a)). Here we choose τ_2 as a bifurcation parameter when $\tau_1 = 0$ (Case IV) and other parameters are the same as in Figure 2. This figure shows that, there is a critical value of the delay parameter τ_2, say $\tau_{2_0} = 1.6079$, below which the system is stable and above this value it is unstable. System experiences Hopf-bifurcation when delay parameter τ_2 crosses its critical value. We also observe that when we change the ratio of death rate of the middle predator and growth rate of the prey (that is, $\omega_5 = a_2/a_1$) from 0.152 to 0.2, surprisingly the delayed system (Cases II–V) becomes asymptotically stable for all permissible $\tau_1, \tau_2 \geq 0$ (see Figure 4). This may be viewed as a case of delay independent stability.

https://doi.org/10.1017/S144618111700044X Published online by Cambridge University Press

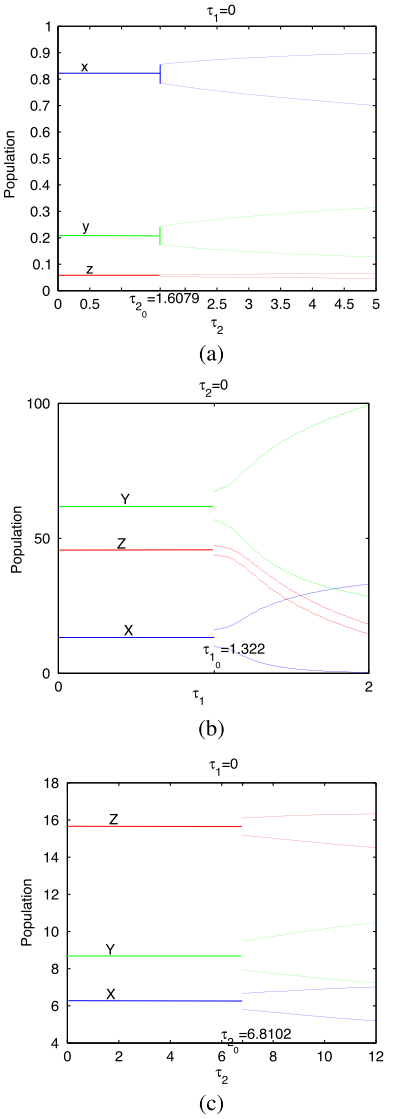

FIGURE 3. Bifurcation diagrams of: (a) system (2.3) with respect to delay parameter τ_2 when $\tau_1 = 0$ (Case IV) with other parameters the same as in Figure 1(a), here system (2.3) is stable when $\tau_2 \in [0, \tau_{2_0} = 1.6079)$, unstable when $\tau_2 > \tau_{2_0} = 1.6079$ and Hopf-bifurcation occurs when $\tau_2 = \tau_{2_0} = 1.6079$; (b) system (5.1) with respect to delay parameter τ_1 when $\tau_2 = 0$ (Case IV) with other parameters the same as in Figure 1(b), here system (5.1) is stable when $\tau_1 \in [0, \tau_{1_0} = 1.322)$, unstable when $\tau_1 > \tau_{1_0} = 1.322$ and Hopf-bifurcation occurs when $\tau_1 = \tau_{1_0} = 1.322$; (c) system (5.2) with respect to delay parameter τ_2 when $\tau_1 = 0$ (Case IV) with other parameters the same as in Figure 1(c), here system (5.2) is stable when $\tau_2 \in [0, \tau_{2_0} = 6.8102)$, unstable when $\tau_2 > \tau_{2_0} = 6.8102$ and Hopf-bifurcation occurs when $\tau_2 = \tau_{2_0} = 6.8102$.

https://doi.org/10.1017/S144618111700044X Published online by Cambridge University Press

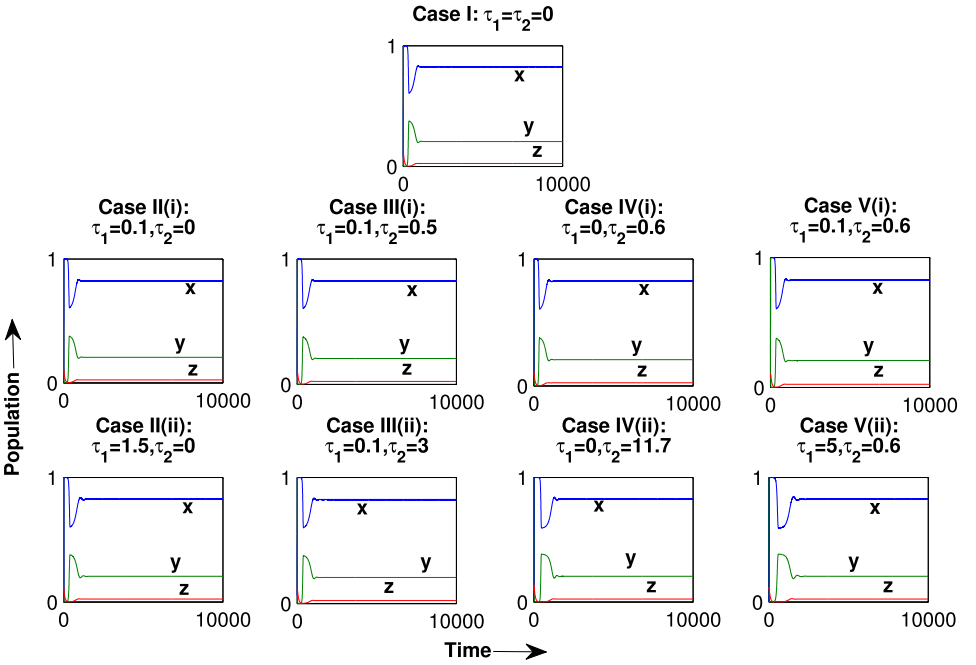

FIGURE 4. Time evolution of system (2.3) with parameter Set_2. For Case I, when $\tau_1 = \tau_2 = 0$, the positive interior equilibrium $E_3(0.8244, 0.2063, 0.024)$ is locally asymptotically stable. For Cases II, III, IV and V, the system remains stable for all possible combinations of $\tau_1, \tau_2 \geq 0$. Parameters are as in the text.

For the same parameter set taken by Upadhyay and Naji [28]

$$\text{Set}_2 : \omega_4 = 0.25, \quad \omega_6 = 0.8, \quad \omega_7 = 0.25, \quad \omega_8 = 0.01,$$
$$\omega_9 = 0.1, \quad \omega_{10} = 0.28, \quad \omega_{11} = 0.06, \quad \omega_{12} = 0.25,$$

we have plotted the bifurcation diagrams (Figure 5) with respect to the parameter ω_5 for the populations y (panel (a)) and z (panel (b)) of both nondelayed and delayed model system (2.3). The period doubling phenomena started at a higher value of the parameter ω_5 in the bifurcation diagram for the delayed model system compared to the nondelayed model system for both populations y and z. Also, the periodic window of the bifurcation diagram for the nondelayed model system has been observed in the ranges $0.35 < \omega_5 < 0.385$, which splits into two parts in the bifurcation diagram drawn for the delayed model system (for both populations y and z). For the delayed model system, we have taken delays as $\tau_1 = \tau_2 = 0.5$.

Now, we consider food chain models with BD and HV type functional responses in place of a CM type functional response, and study how it affects the overall dynamics of the model system.

https://doi.org/10.1017/S144618111700044X Published online by Cambridge University Press

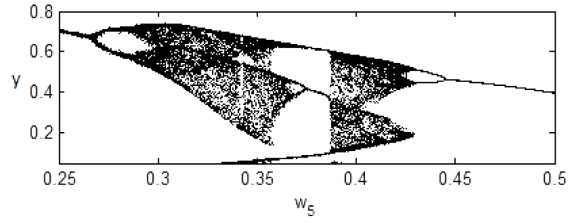

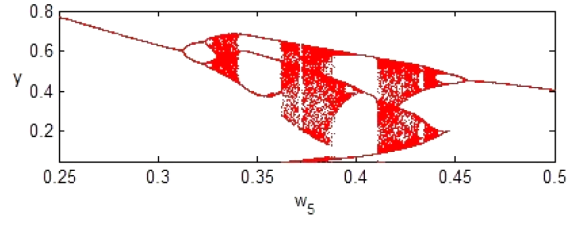

(a)

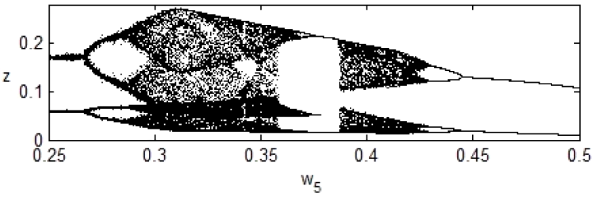

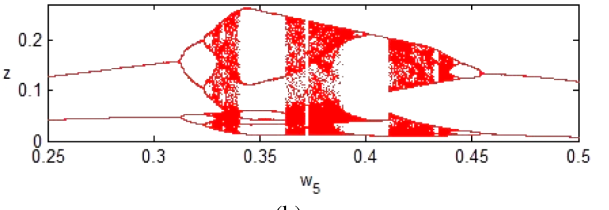

(b)

FIGURE 5. Bifurcation diagram for populations y and z in (a) and (b), respectively, of system (2.3) with varying ω_5. Black diagrams (online) are for $\tau_1 = \tau_2 = 0$ and red diagrams (online) are for $\tau_1 = \tau_2 = 0.5$. The rest of the parameters are the same as given in the text as parameter Set_2.

5.1. Dynamics of the model system having Holling type II and BD type functional responses

The model equations are

$$\begin{aligned}
\frac{dX}{dT} &= a_1 X\left(1 - \frac{X}{K}\right) - \frac{\omega_0 XY}{X + D}, \\
\frac{dY}{dT} &= -a_2 Y + \frac{\omega_1 X(T-\tau_1)Y(T-\tau_1)}{X(T-\tau_1) + D_1} - \frac{\omega_2 YZ}{Y + bZ + D_2}, \\
\frac{dZ}{dT} &= -a_3 Z + \frac{\omega_3 Y(T-\tau_2)Z(T-\tau_2)}{Y(T-\tau_2) + bZ(T-\tau_2) + D_2},
\end{aligned} \tag{5.1}$$

https://doi.org/10.1017/S144618111700044X Published online by Cambridge University Press

where D_2 and b represent the protection provided to the intermediate predator by its environment and intensity of interference between individuals of the top predator, respectively. For finding out the analytical stability conditions of system (5.1), symbolically (3.1)–(3.18) are the same for all calculations of this model and the Jacobian matrix has the following entities:

$$A_1 = X^* + D = X^* + D_1, \quad B_1 = Y^* + bZ^* + D_2, \quad a_{11} = \frac{w_0 X^* Y^*}{A_1^2} - \frac{a_1 X^*}{K},$$

$$a_{12} = -\frac{w_0 X^*}{A_1}, \quad a_{22} = -a_2 - \frac{w_2 Z^*(bZ^* + D_2)}{B_1^2}, \quad a_{23} = -\frac{w_2 Y^*(Y^* + D_2)}{B_1^2},$$

$$a_{33} = -a_3, \quad b_{21} = \frac{w_1 D_1 Y^*}{A_1^2}, \quad b_{22} = \frac{w_1 X^*}{A_1},$$

$$c_{32} = \frac{w_3 Z^*(bZ^* + D_2)}{B_1^2}, \quad c_{33} = \frac{w_3 Y^*(Y^* + D_2)}{B_1^2}.$$

We perform numerical computations to observe various dynamics of the coexistence equilibrium point $E^*(X^*, Y^*, Z^*)$ for the model system (5.1). We consider the fixed parameter values as

$$\text{Set}_3 : a_1 = 1, \quad K = 50, \quad \omega_0 = 0.75, \quad D = 50, \quad a_2 = 0.05, \quad \omega_1 = 0.6, \quad D_1 = 50,$$
$$\omega_2 = 0.2, \quad D_2 = 50, \quad b = 0.25, \quad a_3 = 0.06, \quad \omega_3 = 0.12.$$

By using this parameter set, we find the coexistence abundance is $X^* = 13.408, Y^* = 61.8334, Z^* = 47.5221$. First we observe the two-dimensional bifurcation scenario of system (5.1) in the $\tau_1\tau_2$-plane (Figure 1(b)). On the red line in the τ_1-axis, the system is unstable and in the rest of the $\tau_1\tau_2$-plane the system is stable. Also, when τ_1 crosses the critical value $\tau_{1_0} = 1.322$, the system possesses Hopf-bifurcation. These two different characteristic dynamical phenomena are presented numerically in this section. We show five different numerical examples corresponding to five analytical results (Cases (I)–(V), see Table 2).

(i) For Case I, first we consider the nondelayed system of (5.1), that is when $\tau_1 = \tau_2 = 0$, then $\mu_1 = 0.0808 > 0, \mu_2 = 0.0713 > 0$ and $\Delta = 0.0051$. In this case the system is asymptotically stable (Figure 6 (Case I)).

(ii) For Case II, $(C + I)^2 - (F + K)^2 = -2.8749 \times 10^{-8} < 0$, so the parameter set satisfies the conditional stability condition. Here, $\omega_0 = 0.2456$ and $\tau_{1_0} = 1.322$. In this case the system is asymptotically stable for $\tau_1 = 0.7 < \tau_{1_0} = 1.322$ (Figure 6 (Case II(i))) and unstable for $\tau_1 = 1.5 > \tau_{1_0} = 1.322$ (Figure 6 (Case II(ii))). The system experiences Hopf-bifurcation when the delay parameter τ_1 crosses its critical value $\tau_{1_0} = 1.322$.

https://doi.org/10.1017/S144618111700044X Published online by Cambridge University Press

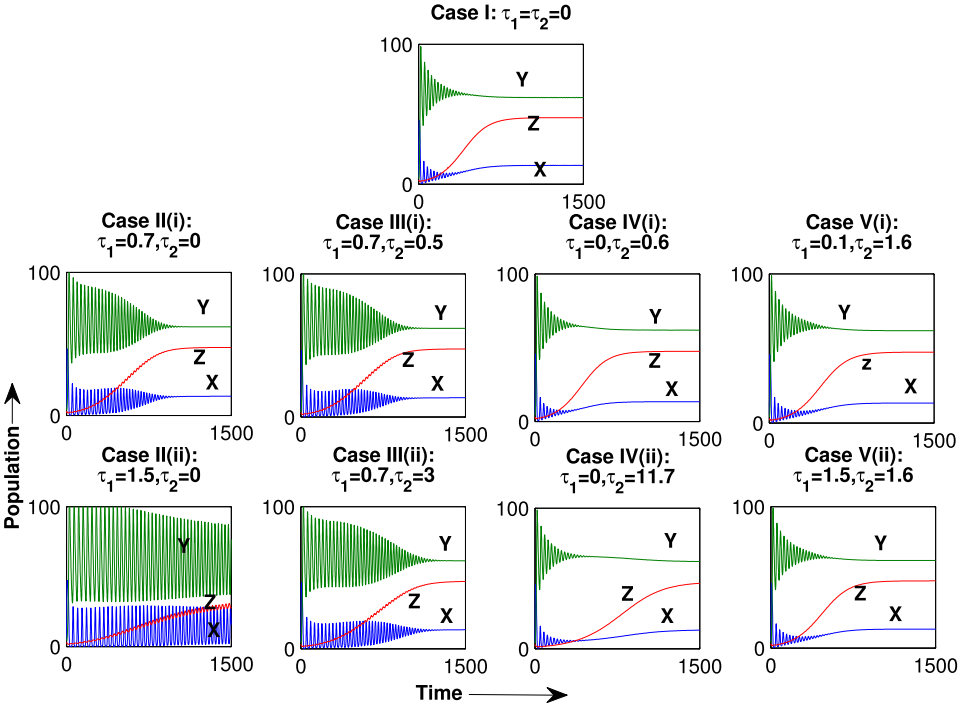

FIGURE 6. Time evolution of system (5.1) with parameter Set_3. For Case I, when $\tau_1 = \tau_2 = 0$, the positive interior equilibrium $E_3(13.408, 61.8334, 47.5221)$ is locally asymptotically stable. For Case II ($\tau_2 = 0$), the system remains stable for $\tau_1 = 0.7 < \tau_{1_0} = 1.322$. Similarly for Case III, the system is stable for all $\tau_2 \geq 0$ by choosing $\tau_1 = 0.7$. For Case IV ($\tau_1 = 0$), the system remains stable for all $\tau_2 \geq 0$ and finally for Case V, the system is stable for all $\tau_1, \tau_2 \geq 0$. Parameters are as in the text.

(iii) For Case III, it follows that $(C + I)^2 - (F + K)^2 = -2.8749 \times 10^{-8} < 0, (C + F)^2 - (I + K)^2 = 4.8354 \times 10^{-6} > 0$, so the parameter set does not satisfy the conditional stability criteria. In this case the system is asymptotically stable for all $\tau_2 \geq 0$ while $\tau_1 \in [0, \tau_{1_0})$ (Figure 6 (Case III(i)): $\tau_1 = 0.7, \tau_2 = 0.5$ and Figure 6 (Case III(ii)): $\tau_1 = 0.7, \tau_2 = 3$).

(iv) For Case IV, the expression $(C + F)^2 - (I + K)^2 = 4.8354 \times 10^{-6} > 0$, the parameter set does not satisfy the conditional stability criteria. In this case the system is asymptotically stable for all $\tau_2 > 0$ (Figure 6 (Case IV(i)): $\tau_1 = 0, \tau_2 = 0.6$ and Figure 6 (Case IV(ii)): $\tau_1 = 0, \tau_2 = 11.7$).

(v) For Case V, it turns out that $(C + I)^2 - (F + K)^2 = -2.8749 \times 10^{-8} < 0, (C + F)^2 - (I + K)^2 = 4.8354 \times 10^{-6} > 0$, so the parameter set does not satisfy the conditional stability criteria. In this case the system is asymptotically stable for all $\tau_1, \tau_2 \geq 0$ (Figure 6 (Case V(i)): $\tau_1 = 0.1, \tau_2 = 1.6$ and Figure 6 (Case V(ii)): $\tau_1 = 1.5, \tau_2 = 1.6$).

https://doi.org/10.1017/S144618111700044X Published online by Cambridge University Press

TABLE 2. Stability results of system (5.1) with parameter Set_3.

Case	Condition	Critical value	Delay value	Status	Figure 8
I	$\mu_1 = 0.0808 > 0$, $\mu_2 = 0.0713 > 0$, $\Delta = 0.0051$	NA	NA	Stable	Case I
II	$\Sigma = -2.8749 \times 10^{-8} < 0$, with condition of Case I	$\omega_0 = 0.2456$ $\tau_{1_0} = 1.322$	$\tau_1 = 0.7, \tau_2 = 0$ $\tau_1 = 1.5, \tau_2 = 0$	Stable Unstable	Case II(i) Case II(ii)
III	$\Sigma = -2.8749 \times 10^{-8} < 0$, $\Psi = 4.8354 \times 10^{-6} > 0$, with condition of Case I	NA	$\tau_1 = 0.7, \tau_2 = 0.5$ $\tau_1 = 0.7, \tau_2 = 3$	Stable Stable	Case III(i) Case III(ii)
IV	$\Psi = 4.8354 \times 10^{-6} > 0$, with condition of Case I	NA	$\tau_1 = 0, \tau_2 = 0.6$ $\tau_1 = 0, \tau_2 = 11.7$	Stable Stable	Case IV(i) Case IV(ii)
V	$\Sigma = -2.8749 \times 10^{-8} < 0$, $\Psi = 4.8354 \times 10^{-6} > 0$, with condition of Case I	NA	$\tau_1 = 0.1, \tau_2 = 1.6$ $\tau_1 = 1.5, \tau_2 = 1.6$	Stable Stable	Case V(i) Case V(ii)

We can verify the previous results by observing the bifurcation diagram (Figure 3(b)), here we choose τ_1 as a bifurcation parameter when $\tau_2 = 0$ (Case II) and other parameters are as in Figure 6. This figure shows that, there is a critical value of the delay parameter τ_1, say $\tau_{1_0} = 1.322$, below which the system is stable and above the system is unstable. The system experiences Hopf-bifurcation when delay parameter τ_1 crosses its critical value.

Again, we consider the fixed parameter values as

$$\text{Set}_4: a_1 = 1, \quad K = 50, \quad \omega_0 = 0.7, \quad D = 5, \quad a_2 = 0.25, \quad \omega_1 = 0.5, \quad D_1 = 5,$$
$$\omega_2 = 0.5, \quad D_2 = 1, \quad b = 0.25, \quad a_3 = 0.06, \quad \omega_3 = 0.25.$$

Using this parameter set, show the effect of delays on the dynamics of the model system (5.1). It is interesting to see the role of the delays on the dynamics of the model system (5.1) as we all know that delay destabilizes the system in general, but here we observed that delay reduces the chaotic system in limit cycle as well as in stable mode. It is clearly shown in Figure 7(a)–(f), how the dynamic behaviour of the system is affected by single or multiple delays. In Figure 7(a), we have shown that the nondelayed (τ_1 and $\tau_2 = 0$) model system (5.1) exhibits chaotic dynamics. If we consider single delay τ_1 (taking $\tau_2 = 0$), the chaotic behaviour changes to limit cycle as well as stable focus due to variation of τ_1 from $\tau_1 = 7.35$ to $\tau_1 = 10$ (Figure 7(b) and (c)) and if we consider τ_2 only (taking $\tau_1 = 0$), the system remains in chaotic state for $\tau_2 = 1$ (Figure 7(d)) or changes to limit cycle for $\tau_2 = 15$ (Figure 7(e)). Also, the system shows stable behaviour due to multiple delays, when $\tau_1 = 10$ and $\tau_2 = 1$ (Figure 7(f)).

https://doi.org/10.1017/S144618111700044X Published online by Cambridge University Press

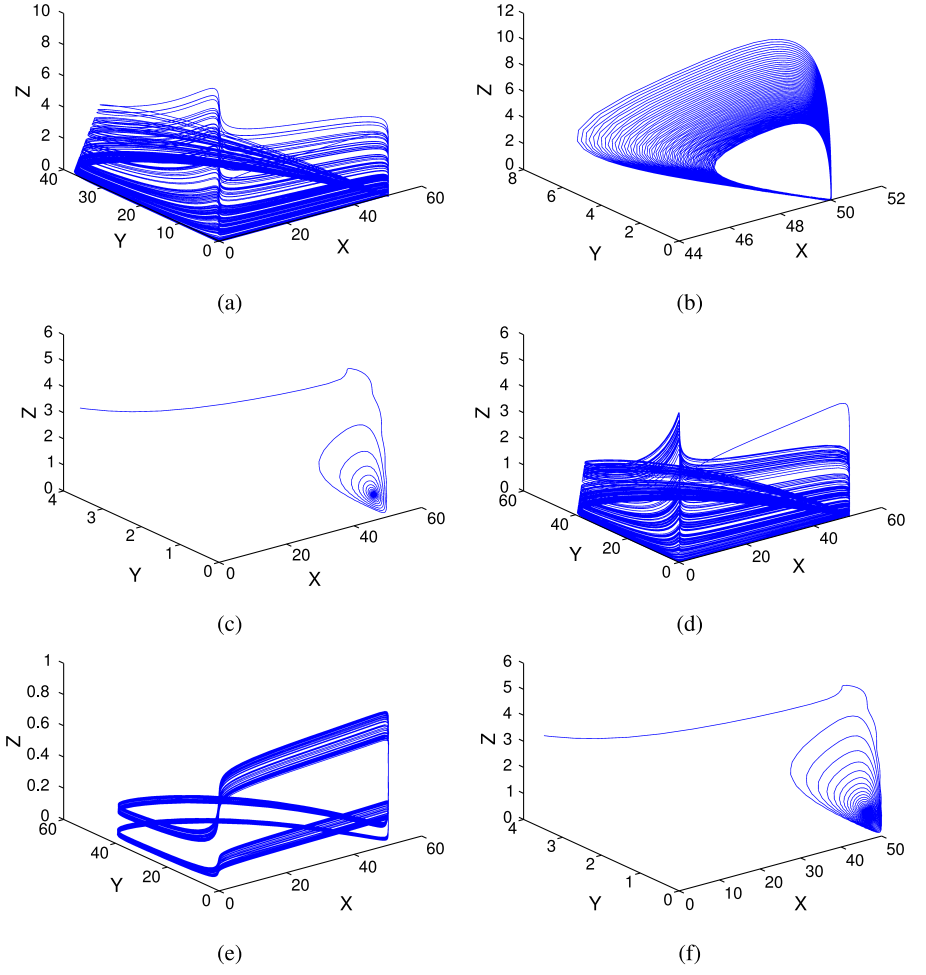

FIGURE 7. Phase plot diagram of system (5.1) for different combination of τ_1 and τ_2: (a) $\tau_1 = 0, \tau_2 = 0$, (b) $\tau_1 = 7.35, \tau_2 = 0$, (c) $\tau_1 = 10, \tau_2 = 0$, (d) $\tau_1 = 0, \tau_2 = 1$, (e) $\tau_1 = 0, \tau_2 = 15$, (f) $\tau_1 = 10, \tau_2 = 1$. The rest of the parameters are taken as given in the text.

5.2. Dynamics of the model system having Holling type II and HV type of functional responses We consider the following system

$$\begin{aligned}
\frac{dX}{dT} &= a_1 X\left(1 - \frac{X}{K}\right) - \frac{\omega_0 XY}{X + D}, \\
\frac{dY}{dT} &= -a_2 Y + \frac{\omega_1 X(T - \tau_1) Y(T - \tau_1)}{X(T - \tau_1) + D_1} - \frac{\omega_2 YZ}{mZ^\gamma + Y}, \\
\frac{dZ}{dT} &= -a_3 Z + \frac{\omega_3 Y(T - \tau_2) Z(T - \tau_2)}{m(Z(T - \tau_2))^\gamma + Y(T - \tau_2)},
\end{aligned} \tag{5.2}$$

https://doi.org/10.1017/S144618111700044X Published online by Cambridge University Press

where m and γ are half saturation constants and the Hassell–Varley constant [33], respectively. For finding out the analytical stability conditions of system (5.2), symbolically (3.1)–(3.18) are the same for all calculations of this model and the Jacobian matrix has the following entities:

$$A_1 = X^* + D = X^* + D_1, \quad B_1 = Y^* + mZ^\gamma, \quad a_{11} = \frac{w_0 X^* Y^*}{A_1^2} - \frac{a_1 X^*}{K}$$

$$a_{12} = -\frac{w_0 X^*}{A_1}, \qquad a_{22} = -a_2 - \frac{w_2 m Z^{*(\gamma+1)}}{B_1^2},$$

$$a_{23} = -\frac{w_2 m Y^* Z^{*\gamma}(1-\gamma) + w_2 Y^*}{B_1^2}, \quad a_{33} = -a_3,$$

$$b_{21} = \frac{w_1 D_1 Y^*}{A_1^2}, \qquad b_{22} = \frac{w_1 X^*}{A_1},$$

$$c_{32} = \frac{w_3 m Z^{*(\gamma+1)}}{B_1^2}, \qquad c_{33} = \frac{w_3 m Y^* Z^{*\gamma}(1-\gamma) + w_3 Y^{*2}}{B_1^2}.$$

We perform numerical computations to observe various dynamics of the coexistence equilibrium point $E^*(X^*, Y^*, Z^*)$ for the model system (5.2). We consider the fixed parameter values as

$$\text{Set}_5: a_1 = 1, \quad K = 10, \quad \omega = 0.7, \quad D = 10, \quad a_2 = 0.05, \quad \omega_1 = 0.6, \quad D_1 = 10,$$
$$\omega_2 = 0.2, \quad m = 5, \quad \gamma = 0.2, \quad a_3 = 0.06, \quad \omega_3 = 0.12.$$

By using this parameter set, the coexistence abundance is $X^* = 5.2673$, $Y^* = 8.6743$, $Z^* = 15.7146$. First we observe the two-dimensional bifurcation scenario of the system (5.2) in the $\tau_1\tau_2$-plane (Figure 1(c)). On the red line in the τ_2-axis the system is unstable, and in the rest of the $\tau_1\tau_2$-plane the system is stable. Also, when τ_2 crosses the critical value $\tau_{2_0} = 6.8102$, the system experiences Hopf-bifurcation. These two different characteristic dynamical phenomena are presented numerically in this section. We show five different numerical examples corresponding to five analytical results (Cases (I)–(V), see Table 3).

(i) For Case I, first we consider the nondelayed system of (5.2), that is when $\tau_1 = \tau_2 = 0$, then $\mu_1 = 0.3983 > 0, \mu_2 = 0.0165 > 0$ and $\Delta = 0.0042$. In this case the system is asymptotically stable (Figure 8 (Case I)).

(ii) For Case II, $(C + I)^2 - (F + K)^2 = 7.5464 \times 10^{-6} > 0$, so the parameter set does not satisfy the conditional stability criteria. In this case the system is asymptotically stable for all $\tau_1 > 0$ (Figure 8 (Case II(i)): $\tau_1 = 0.4$ and Figure 8 (Case II(ii)): $\tau_1 = 1.5$).

(iii) For Case III, it follows that $(C + I)^2 - (F + K)^2 = 7.5464 \times 10^{-6} > 0$, $(C + F)^2 - (I + K)^2 = -3.1483 \times 10^{-6} < 0$, so the parameter set does not satisfy the conditional stability criteria. In this case the system is asymptotically stable for all $\tau_1, \tau_2 \geq 0$ (Figure 8 (Case III(i)): $\tau_1 = 0.4, \tau_2 = 1.6$ and Figure 8 (Case III(ii)): $\tau_1 = 0.4, \tau_2 = 7.7$).

https://doi.org/10.1017/S144618111700044X Published online by Cambridge University Press

Table 3. Stability results of system (5.2) with parameter Set$_5$.

Case	Condition	Critical value	Delay value	Status	Figure 12
I	$\mu_1 = 0.3983 > 0$, $\mu_2 = 0.0165 > 0$, $\Delta = 0.0042$	NA	NA	NA	Case I
II	$\Sigma = 7.5464 \times 10^{-6} > 0$, with condition of Case I	NA	$\tau_1 = 0.4, \tau_2 = 0$	Stable	Case II(i)
			$\tau_1 = 1.5, \tau_2 = 0$	Stable	Case II(ii)
III	$\Sigma = 7.5464 \times 10^{-6} > 0$, $\Psi = -3.1483 \times 10^{-6} < 0$, with condition of Case I	NA	$\tau_1 = 0.4, \tau_2 = 0.5$	Stable	Case III(i)
			$\tau_1 = 0.4, \tau_2 = 2.7$	Stable	Case III(ii)
IV	$\Psi = -3.1483 \times 10^{-6} < 0$, with condition of Case I	$\omega_0 = 0.0661$, $\tau_{2_0} = 6.8102$	$\tau_1 = 0, \tau_2 = 1.6$	Stable	Case IV(i)
			$\tau_1 = 0, \tau_2 = 7.7$	Unstable	Case IV(ii)
V	$\Sigma = 7.5464 \times 10^{-6} > 0$, $\Psi = -3.1483 \times 10^{-6} < 0$, with condition of Case I	NA	$\tau_1 = 0.1, \tau_2 = 3.6$	Stable	Case V(i)
			$\tau_1 = 2.5, \tau_2 = 3.6$	Stable	Case V(ii)

(iv) For Case IV, we obtain $(C + F)^2 - (I + K)^2 = -3.1483 \times 10^{-6} < 0$, the parameter set satisfies the conditional stability criteria. Here, $\omega_0 = 0.0661$ and $\tau_{2_0} = 6.8102$. In this case the system is asymptotically stable for $\tau_2 < \tau_{2_0} = 6.8102$ and unstable for $\tau_2 > \tau_{2_0} = 6.8102$ (Figure 8 (Case IV(i)) : $\tau_1 = 0, \tau_2 = 1.6$ and Figure 8 (Case IV(ii)): $\tau_1 = 0, \tau_2 = 7.7$). The system undergoes Hopf-bifurcation when the delay parameter τ_2 crosses its critical value $\tau_{2_0} = 6.8102$.

(v) For Case V, $(C + I)^2 - (F + K)^2 = 7.5464 \times 10^{-6} > 0$, $(C + F)^2 - (I + K)^2 = -3.1483 \times 10^{-6} < 0$, so the parameter set does not satisfy the conditional stability condition. In this case, the system is asymptotically stable for all $\tau_1 \geq 0$ while $\tau_2 \in [0, \tau_{2_0})$ (Figure 8 (Case V(i)): $\tau_1 = 0.1, \tau_2 = 3.6$ and Figure 8 (Case V(ii)): $\tau_1 = 2.5, \tau_2 = 3.6$).

We verify the above results from the bifurcation diagram (Figure 3(c)). Here we choose τ_2 as a bifurcation parameter when $\tau_1 = 0$ (Case IV) and other parameters are as in Figure 8. This figure shows that there is a critical value of the delay parameter τ_2, say $\tau_{2_0} = 6.8102$, below which the system is stable and above which the system is unstable. The system experiences Hopf-bifurcation when the delay parameter τ_2 crosses its critical value.

Again, we consider the fixed parameter values as

$$\text{Set}_6: a_1 = 1, \quad K = 20, \quad \omega = 0.7, \quad D = 10, \quad a_2 = 0.05, \quad \omega_1 = 0.6, \quad D_1 = 10, \\ \omega_2 = 0.2, \quad m = 5, \quad \gamma = 0.2, \quad a_3 = 0.06, \quad \omega_3 = 0.12.$$

The effect of delays on the dynamics of the model system (5.2) are shown by using this parameter set. Again, we observe that the dynamics of the model system is affected

https://doi.org/10.1017/S144618111700044X Published online by Cambridge University Press

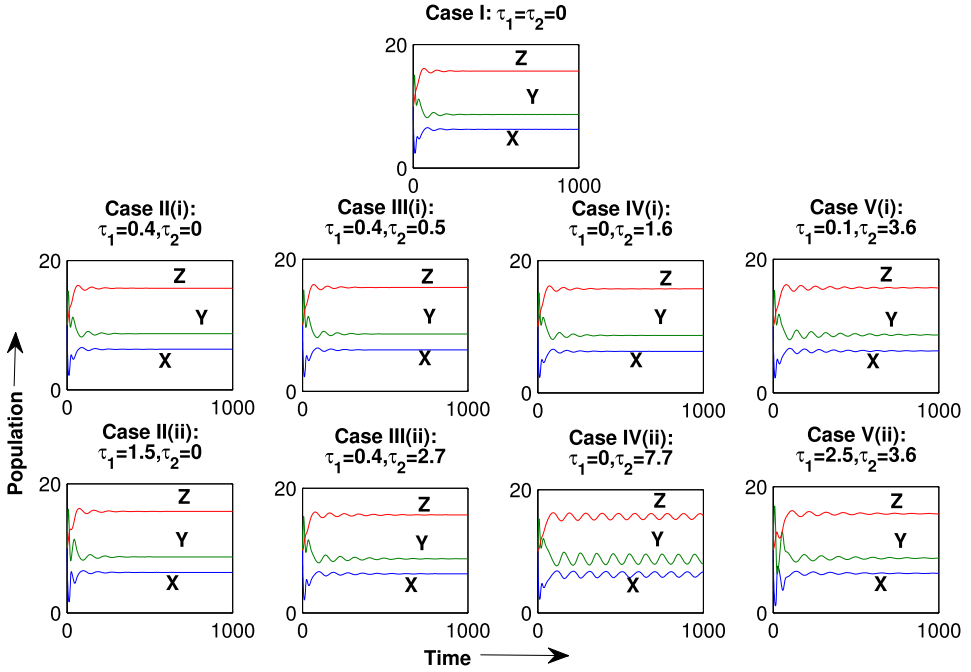

FIGURE 8. Time evolution of system (5.2) with parameter Set_5. For Case I, when $\tau_1 = \tau_2 = 0$, the positive interior equilibrium $E_3(6.2673, 8.6743, 15.7146)$ is locally asymptotically stable. For Case II ($\tau_2 = 0$), the system remains stable for all $\tau_1 > 0$. Similarly for Case III, the system is stable for all $\tau_1, \tau_2 > 0$. For Case IV ($\tau_1 = 0$), the system remains stable for $\tau_2 = 1.6 < \tau_{2_0} = 6.81020$ and unstable for $\tau_2 = 7.7 > \tau_{2_0} = 6.8102$ and finally for Case V, the system is stable for all $\tau_1 \geq 0$ by choosing $\tau_2 = 3.6$. Parameters are as in the text.

by single or multiple delays. The chaotic dynamic behaviour of the nondelayed (τ_1 and $\tau_2 = 0$, see Figure 9(a)) model system (5.2) changes to limit cycle behaviour due to the presence of any single (τ_1 or $\tau_2 = 0$) or both the delays (τ_1 and $\tau_2 \neq 0$) in Figure 9. The system reduces to limit cycle in all three combinations of delays, that is, when (i) $\tau_1 = 1$ and $\tau_2 = 0$ (Figure 9(b)), (ii) $\tau_1 = 0$ and $\tau_2 = 1.66$ (Figure 9(c)) and (iii) $\tau_1 = 1$ or $\tau_2 = 1$ (Figure 9(d)).

6. Discussion and conclusions

In this work, the dynamic behaviour of a three-species food chain model incorporating multiple time delays has been studied. The interaction between the prey and an intermediate predator follows the HT II functional response, and that between the top predator and its prey (middle predator) has been taken as a mutual interference type functional response. The dynamics of the model system has been analysed for all the functional responses considered. We also studied the effect of gestation delays, τ_1 and τ_2, on the considered model systems, and observed very interesting results in all

https://doi.org/10.1017/S144618111700044X Published online by Cambridge University Press

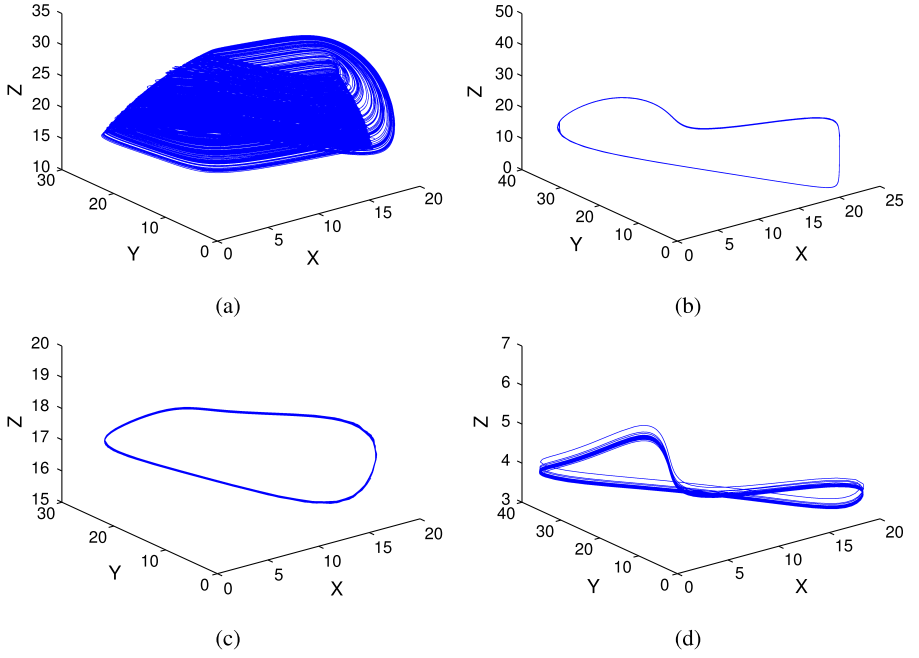

FIGURE 9. Phase plot diagram of system (5.2) for different combination of τ_1 and τ_2: (a) $\tau_1 = 0, \tau_2 = 0$, (b) $\tau_1 = 1, \tau_2 = 0$, (c) $\tau_1 = 0, \tau_2 = 1.66$, (d) $\tau_1 = 1, \tau_2 = 1$. The rest of the parameters are taken as given in the text.

cases of the multiple delays. We have carried out numerical simulations to realize the quantitative effect of both delays in the given ranges. For different parameter sets, we find different dynamics of the model systems.

First, we have studied the dynamics of the model system with CM functional response. For a particular set, we obtain a critical value of τ_2, that is, $\tau_{2_0} = 1.6079$ at which the system experiences Hopf-bifurcation, whereas for some other parameter sets, we find that the system remains stable for all values of $\tau_1, \tau_2 \geq 0$. This clearly indicates that the incorporation of gestation delay τ_2 in the top predator z, is more effective than the gestation delay, τ_1 in the middle predator y. Choosing the death rate of the intermediate predator, that is, ω_5 as a bifurcation parameter, the analysis is carried out. The bifurcation diagram for populations y and z with respect to ω_5 is obtained for two cases, taking $\tau_1 = \tau_2 = 0$ and $\tau_1 = \tau_2 = 0.5$. We observe that the periodic window splits into two parts for both populations y and z. We have derived the explicit formulae which determine the stability, direction and period of the bifurcating periodic solutions by normal form theory and centre manifold reduction with respect to τ_1 for fixed $\tau_2 \in (0, \tau_{2_0})$. It is also shown that the positive equilibria of the system remains stable under certain conditions.

It is interesting to see the effect of delays with different functional responses. When we analysed the model system with BD functional response, we observed that delay

https://doi.org/10.1017/S144618111700044X Published online by Cambridge University Press

stabilizes the model system in the future, despite destabilization. Chaotic dynamic behaviour of the nondelayed model system reduces to limit cycle (for $\tau_1 = 7.35, \tau_2 = 0$ and $\tau_1 = 0, \tau_2 = 15$) as well as stable focus (for $\tau_1 = 10, \tau_2 = 0$ and $\tau_1 = 10, \tau_2 = 1$) with respect to the different values of the delays τ_1 and τ_2. Whereas chaotic dynamic behaviour of the nondelayed model system changes to only limit cycle (for $\tau_1 = 1, \tau_2 = 0$; $\tau_1 = 0, \tau_2 = 1.66$; $\tau_1 = 1, \tau_2 = 1$) bahaviour for all the possible combinations of τ_1 and τ_2 while studying the model system with HV functional response. For some particular sets, we obtain a critical value of τ_1, that is, $\tau_{1_0} = 1.322$ at which the system experiences Hopf-bifurcation for the model system with BD functional response, and the system with HV functional response experiences Hopf-bifurcation for τ_2, that is, $\tau_{2_0} = 6.8012$.

The role of time delays on all of the three discussed models is significant in the presence of different functional responses. Since this is a hybrid food chain model and we have shown the effect of both time delays with different functional responses in the middle and top predators of the systems, the findings are interesting from the application point of view.

Acknowledgements

The authors wish to thank the anonymous reviewers for many useful suggestions. Rao's research is supported by the Foundation for Scientific Research and Technological Innovation (FSRTI) – A constituent division of Sri Vadrevu Seshagiri Rao Memorial Charitable Trust, Hyderabad, India.

Supplementary material

Supplementary material is available at doi:10.1017/S144618111700044X.

References

[1] R. Agrawal, D. Jana, R. K. Upadhyay and V. Sree Hari Rao, "Complex dynamics of sexually reproductive generalist predator and gestation delay in a food chain model: double Hopf-bifurcation to chaos", *J. Appl. Math. Comput.* **55** (2017) 513–547; doi:10.1007/s12190-016-1048-1.

[2] J. R. Beddington, "Mutual interference between parasites or predators and its effect on searching efficiency", *J. Animal Ecol.* **51** (1975) 331–340; doi:10.2307/3866.

[3] C. Cosner, D. L. DeAngelis, J. S. Ault and D. B. Olson, "Effects of spatial grouping on the functional response of predators", *Theor. Popul. Biol.* **56** (1999) 65–75; doi:10.1006/tpbi.1999.1414.

[4] P. H. Crowley and E. K. Martin, "Functional responses and interference within and between year classes of a dragonfly population", *J. North Am. Benth. Soc.* **8** (1989) 211–221; doi:10.2307/1467324.

[5] D. L. DeAngelis, R. A. Goldstein and R. V. O'eill, "A model for trophic interaction", *Ecology* **56** (1975) 881–892; doi:10.2307/1936298.

[6] B. Dennis, R. Desharnais, J. Cushing, S. Henson and R. Costantino, "Can noise induce chaos?", *Oikos* **102** (2003) 329–339; http://www.jstor.org/stable/3548035.

[7] S. Gakkhar and R. Naji, "Seasonally perturbed prey-predator system with predator-dependent functional response", *Chaos Solitons Fractals* **18** (2003) 1075–1083; doi:10.1016/S0960-0779(03)00075-4.
[8] S. Gakkhar and A. Singh, "Complex dynamics in a prey predator system with multiple delays", *Commun. Nonlinear Sci. Numer. Simul.* **17** (2012) 914–929; doi:10.1016/j.cnsns.2011.05.047.
[9] J. Gao, S. Hwang and J. Liu, "When can noise induce chaos?", *Phys. Rev. Lett.* **82** (1999) 11–32; http://www.jstor.org/stable/3548035.
[10] M. Gao, H. Shi and Z. Li, "Chaos in a seasonally and periodically forced phytoplankton-zooplankton system", *Nonlinear Anal. Real World Appl.* **10** (2009) 1643–1650; doi:10.1016/j.nonrwa.2008.02.005.
[11] J. Guckenheimer and P. Holmes, *Nonlinear oscillations, dynamical systems and bifurcations of vector fields* (Springer, Berlin, 1983).
[12] J. K. Hale, *Theory of functional differential equations*, Volume 3 of *Applied Mathematical Sciences* (Springer, New York, 1977); doi:10.1006/jdeq.2000.3874.
[13] B. D. Hassard, N. D. Kazrinoff and W. H. Wan, *Theory and application of Hopf bifurcation*, Volume 41 of *London Mathematical Society Lecture Note Series* (Cambridge University Press, Cambridge, 1981); doi:10.1137/1024123.
[14] M. P. Hassell and G. C. Varley, "New inductive population model for insect parasites and its bearing on biological control", *Nature* **223** (1969) 1133–1136; doi:10.1038/2231133a0.
[15] G. Huisman and R. J. De Boer, "A formal derivation of the Beddington functional response", *J. Theor. Biol.* **185** (1997) 389–400; doi:10.1006/jtbi.1996.0318.
[16] D. Jana, R. Agrawal and R. K. Upadhyay, "Top-predator interference and gestation delay as determinants of the dynamics of a realistic model food chain", *Chaos Solitons Fractals* **69** (2014) 50–63; doi:10.1016/j.chaos.2014.09.001.
[17] D. Jana, R. Agrawal and R. K. Upadhyay, "Dynamics of generalist predator in a stochastic environment: effect of delayed growth and prey refuge", *Appl. Math. Comput.* **268** (2015) 1072–1094; doi:10.1016/j.amc.2015.06.098.
[18] Y. Kuang, *Delay differential equations with applications in population dynamics* (Academic Press, New York, 1993).
[19] J. van der Meer and B. J. Ens, "Models of interference and their consequences for the spatial distribution of ideal and free predators", *J. Animal Ecol.* **66** (1997) 846–858; http://www.jstor.org/stable/6000.
[20] A. Morozov, S. Petrovskii and B. Li, "Bifurcations and chaos in a predator-prey system with the Allee effect", *Proc. R. Soc. Lond. Ser.* B*: Biol. Sci.* **271** (2004) 1407–1414; doi:10.1098/rspb.2004.2733.
[21] N. Pal, S. Samanta, S. Biswas, M. Alquran, K. Al-Khaled and J. Chattopadhyay, "Stability and bifurcation analysis of a three-species food chain model with delay", *Internat. J. Bifur. Chaos* **25** (2015) 1550123; doi:10.1142/S0218127415501230.
[22] S. Pathak, A. Maiti and G. P. Samanta, "Rich dynamics of a food chain model with Hassell–Varley type functional responses", *Appl. Math. Comput.* **208** (2009) 303–317; doi:10.1016/j.amc.2008.12.015.
[23] S. Ruan, "On nonlinear dynamics of predator-prey models with disc rete delay", *Math. Model. Nat. Phenom.* **4** (2009) 140–188; doi:10.1051/mmnp/20094207.
[24] O. J. Schmitz, "Exploitation in model food chains with mechanistic consumer-resource dynamics", *Theor. Popul. Biol.* **41** (1992) 161–183; doi:10.1016/0040-5809(92)90042-R.
[25] G. T. Skalski and J. F. Gilliam, "Functional responses with predator interference: viable alternatives to the Holling type II model", *Ecology* **82** (2001) 3083–3092; doi:10.1890/0012-9658(2001)082[3083:FRWPIV]2.0.CO;2.
[26] Z. Song, B. Zhen and J. Xu, "Species coexistence and chaotic behavior induced by multiple delays in a food chain system", *Ecol. Compl.* **19** (2014) 9–17; doi:10.1016/j.ecocom.2014.01.004.
[27] K. Tanabe and T. Namba, "Omnivory creates chaos in simple food web models", *Ecology* **86** (2005) 3411–3414; doi:10.1890/05-0720.

[28] R. K. Upadhyay and R. K. Naji, "Dynamics of a three-species food chain model with Crowley–Martin type functional response", *Chaos Solitons Fractals* **42** (2009) 1337–1346; doi:10.1016/j.chaos.2009.03.020.

[29] R. K. Upadhyay, S. N. Raw and V. Rai, "Dynamical complexities in a tritrophic hybrid food chain model with Holling type II and Crowley–Martin functional responses", *Nonlinear Anal. Model. Control* **15** (2010) 361–375; http://www.lana.lt/journal/38/Upadhyay.pdf.

[30] K. Wang, "Periodic solutions to a delayed predator-prey model with Hassell–Varley type functional response", *Nonlinear Anal. Real World Appl.* **12** (2011) 137–145; doi:10.1016/j.nonrwa.2010.06.003.

[31] X. Yang, L. Chen and J. Chen, "Permanence and positive periodic solution for the single species nonautonomous delay diffusive model", *Comput. Math. Appl.* **32** (1996) 109–116; doi:10.1016/0898-1221(96)00129-0.

[32] P. Yodzis and S. Innes, "Body size and consumer resource dynamics", *Amer. Natural.* **139** (1992) 1151–1175; http://www.jstor.org/stable/2462335.

[33] Y. Zhang, S. Gao, K. Fan and Q. Wang, "Asymptotic behavior of a non-autonomous predator-prey model with Hassell–Varley type functional response and random perturbation", *J. Appl. Math. Comput.* **49** (2015) 573–594; doi:10.1007/s12190-014-0854-6.